TPA - TCT
Two Photon Absorption - Transient Current Technique

Moritz Wiehe[1,2], Marcos Fernandez Garcia[1,5], Michael Moll[1], Sebastian Pape[1,6]
Raúl Montero Santos[3], Rogelio Palomo Pinto[4], Ivan Vila Alvarez[5]

[1]CERN
[2]Universität Freiburg
[3]Universidad del Pais Vasco (UPV-EHU)
[4]Universidad de Sevilla (US)
[5]Instituto de Física de Cantabria (CSIC-UC)
[6]Universität Dortmund

38th RD50 workshop
23.06.2021

SPONSORED BY THE
Federal Ministry of Education and Research

Outline

- Intro to TPA-TCT
- Setup
- Power + TPA reference
- Spatial resolution
- Tilt correction

Transient Current Technique

TCT: red laser (650nm = 1.9 eV)
- short penetration depth:
  carriers deposited in a few µm from surface
- front and back TCT: study electron and hole drift
- 2D spatial resolution (5-10µm)

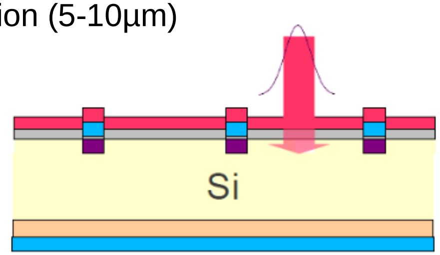

TCT: NIR laser (1064nm = 1.17 eV)
- edge-TCT invented within RD50: 2010
- long penetration depth
- similar to MIPs (though different dE/dx)
- top and edge-TCT
- 2D spatial resolution (5-10µm)

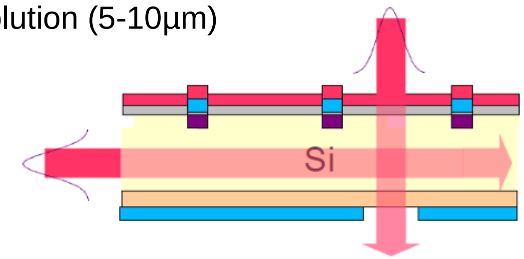

TPA-TCT: SWIR laser (1550nm = 0.8 eV)
- No single photon absorption in silicon
- 2 photons produce one electron-hole pair
- Point-like energy deposition in focal point
- 3D spatial resolution (1 x 1 x 10 mm³)

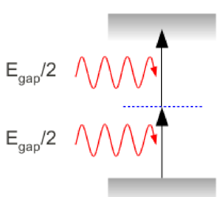

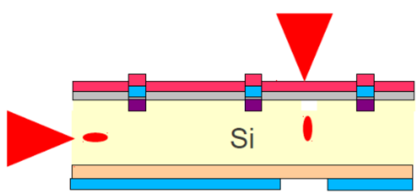

TPA @ UPV/EHU Bilbao
[M. Fernández García, 10.1016/j.nima.2016.05.070]
[M. Fernández García et al 2017 JINST 12 C01038]

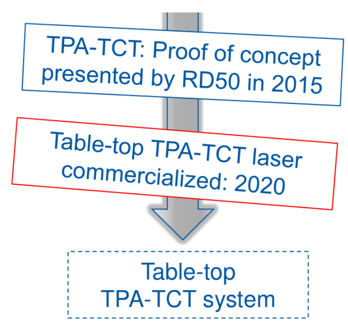

TPA @ CERN
[M. Wiehe, 10.1109/TNS.2020.3044489]

see also: TPA @ ELI
[G.Medin, 36/37thRD50 WS, 2020]

Commercialization (2020)

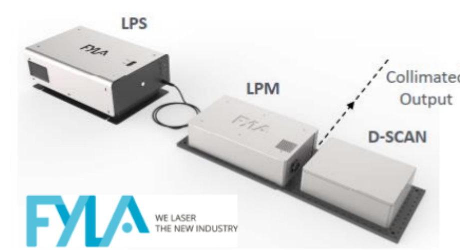

- **LPS: Laser Pulse Source**
  - All-fiber CPA fs pulses generation
  - Pulse rep. single shot to 8 MHz
- **LPM: Laser Pulse Management**
  - Pulse energy: <10 pJ to > 10 nJ
  - Synchronized shutter.
    rise/fall time < 1 us
- **D-SCAN: Dispersion scanning**
  - Pulse duration: 200 fs to 500 fs
  - Spectral and temporal
    pulse characterization

[P.Perez-Millan, Fyla – RD50 Workshop 6/2020]

Two Photon Absorption - TCT

Single Photon Absorption
Continuous energy deposition along beam direction

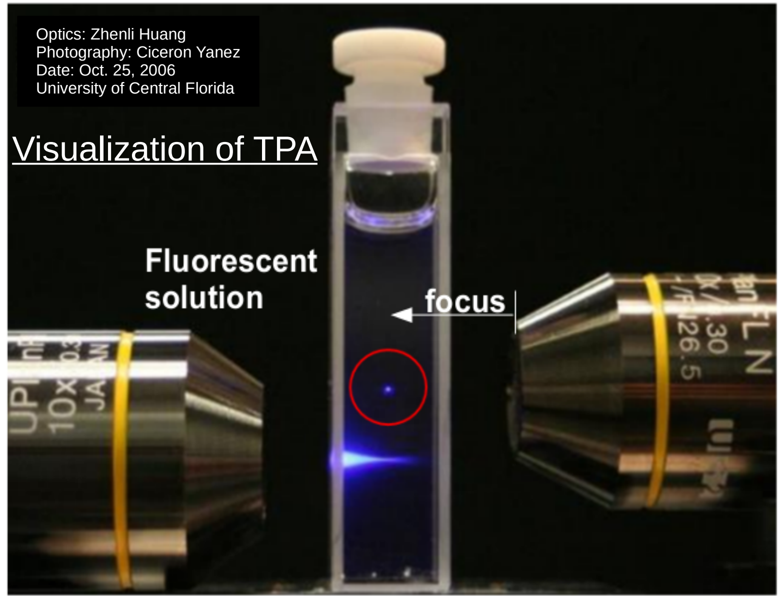

Two Photon Absorption

Absorption only at focal point

Confine photons in **time (femto-second laser)** and in **space (microfocusing)** for Two Photon Absorption

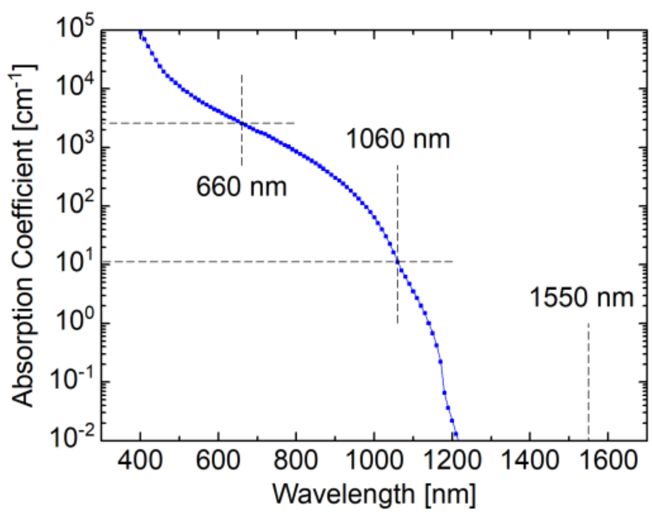

Requirements for TPA-TCT:
- Sub band-gap energy laser
  λ > 1100nm (E < 1.12eV)
- **large enough intensity**

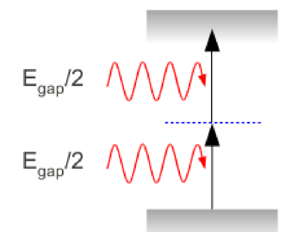

$$\frac{dN(r,z)}{dt} = \frac{\alpha I(r,z)}{\hbar\omega} + \frac{\beta_2 I^2(r,z)}{2\hbar\omega}$$

Carrier Generation equation

Gaussian Laser Beam

Irradiance [I(r,z,t)]=J/m²s

$$I(r,z,t) = \frac{E_p}{\tau}\frac{4\sqrt{\ln 2}}{\pi^{\frac{3}{2}} w^2(z)} \exp\left[-\frac{2r^2}{w^2(z)}\right] \exp\left[-4\ln 2\frac{t^2}{\tau^2}\right]$$

Normalization of I(r,z,t) is such that

$$E_p = \int_{-\infty}^{\infty}\int_0^{2\pi}\int_0^{\infty} I(r,z,t)\, r dr\, d\phi\, dt$$

Ep: Pulse Energy

Gaussian spatial term

Beam radius w $w(z) = w_0\sqrt{1+\left(\frac{\lambda z}{\pi w_0^2 n}\right)^2}$

Rayleigh length z0 $z_0 = \pi w_0^2 n/\lambda$

w is the 2σ radius of the intensity profile and $w(z_0) = \sqrt{2}w_0$

Gaussian temporal term

τ = FWHM pulse temporal width

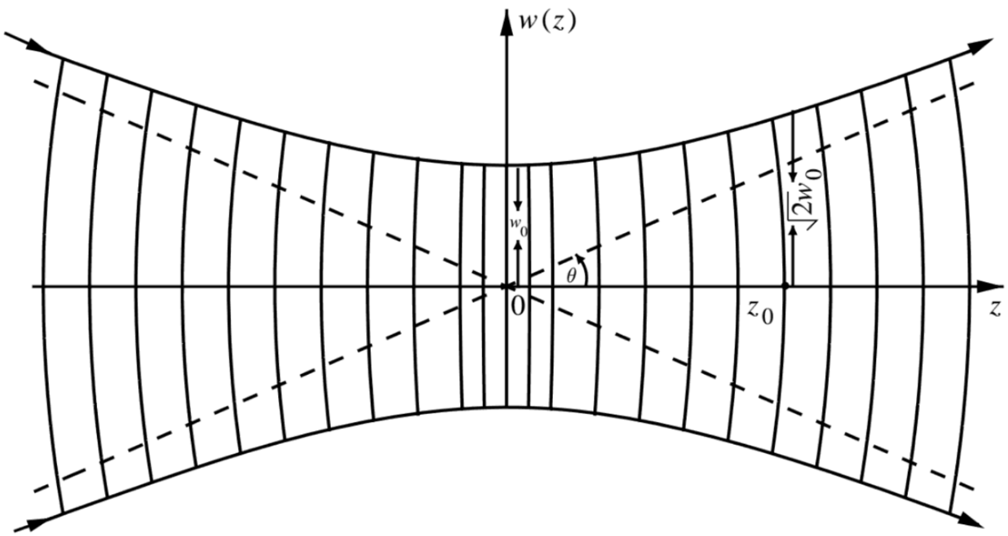

Numerical aperture defined by beam divergence

$$NA = n\sin\theta$$

beam radius w increases linearly at large z

$$\tan\theta = \lim_{z\to\infty}\frac{dw(z)}{dz} = \frac{w_0}{z_0}$$

Two Photon Absorption

Change of irradiance along beam direction **due to absorption** (SPA, TPA, free carrier absorption)

$$\frac{dI(r,z)}{dz} = -\alpha I(r,z) - \beta_2 I^2(r,z) - \sigma_{ex} N I(r,z)$$

linear Term, **SPA**
not contributing
(for unirradiated sensor)

quadratic term, **TPA**

free carrier absorption
neglected

depletion of the beam:

absorbed photons << total flux
beam depletion is **neglected**

$$I(z) = \frac{I_0}{1+\beta_2 I_0 z}$$

creation of charge carriers:

$$\frac{dn(r,z)}{dt} = \frac{\beta_2}{2\hbar\omega} I^2(r,z,t)$$

inserting irradiance (Gaussian beam),
integration over time
→ **charge carrier density**:

$$n_{tpa}(r,z) = \frac{E_p^2 \beta_2 \, 4\ln 2}{\tau\,\hbar\omega\,\pi^{\frac{5}{2}} w^4(z)\,\sqrt{\ln 4}} \exp\left[-\frac{4r^2}{w^2(z)}\right]$$

spatial integration
→ **total number of charge carriers**:

$$N_{tpa} = \int_V n_{tpa}(r,z)\,dV = \frac{E_p^2 n \beta_2 \sqrt{\ln 4}}{4\hbar c \tau \sqrt{\pi}}$$

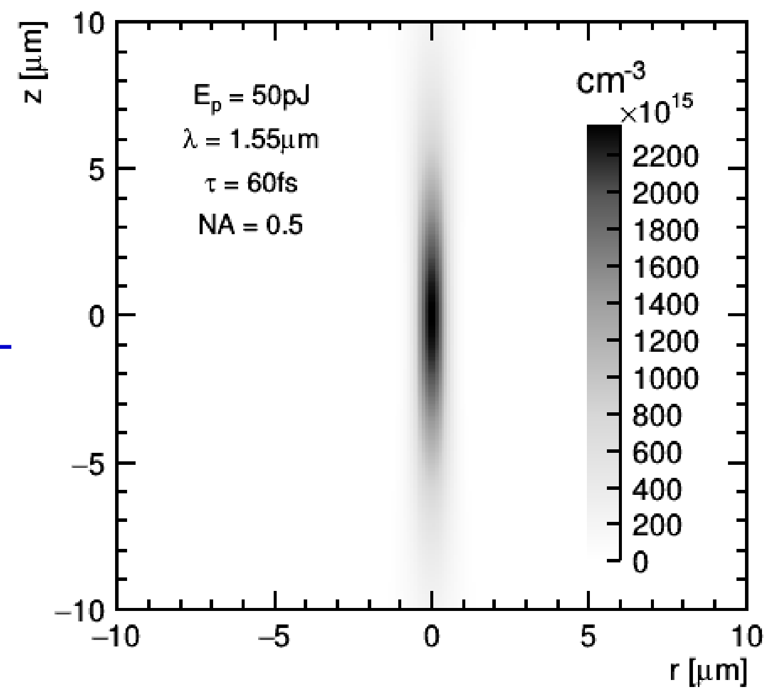

Charge carrier density in silicon β2 = 1.5cm/GW

Pulse width

$$\frac{dI(r,z,t)}{dz} = \underline{-\alpha I(r,z,t)} - \boxed{\beta_2 I^2(r,z,t)} - \sigma_{ex} N I(r,z,t)$$

α = 0 only for <u>non-irradiated</u> silicon

$$n_{tpa}(r,z) = \frac{E_p^2\,\beta_2\,4\ln 2}{\tau\,\hbar\omega\,\pi^{\frac{5}{2}}\,w^4(z)\,\sqrt{\ln 4}} \exp\left[-\frac{4r^2}{w^2(z)}\right]$$

Irradiation:
α ≠ 0 → SPA

$$\frac{n_{tpa}}{n_{spa}} \propto \frac{1}{\tau}$$

FWHM of intensity vs. time profile

- **Best signal resolution for short pulses.**
- **Lower limit given by dispersion: 60fs**

J. Appl. Phys. 110, 011301 (2011);
https://doi.org/10.1063/1.3592270

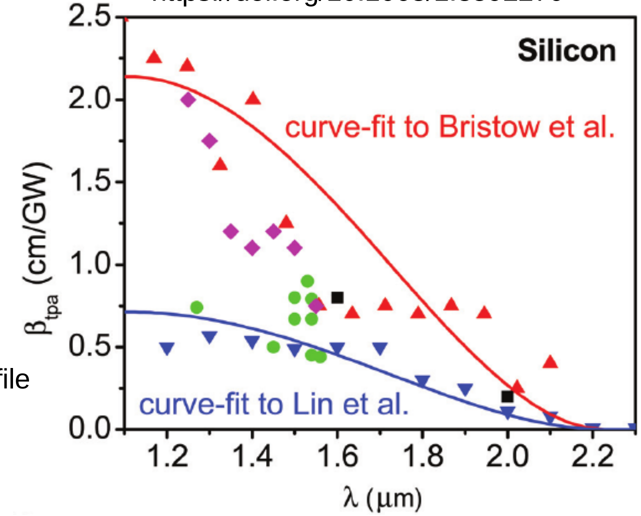

Dispersion in silicon

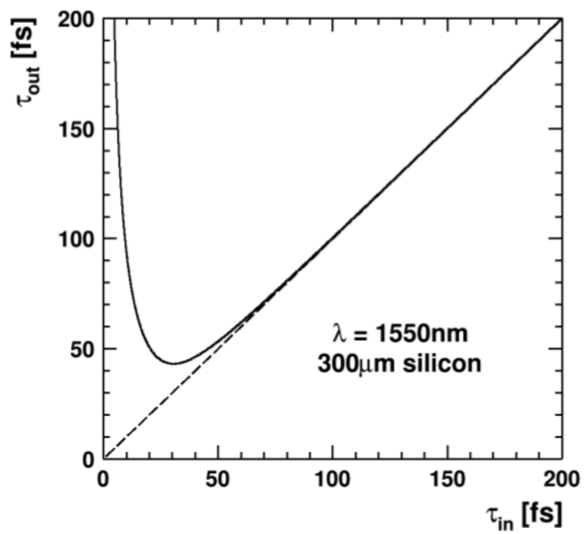

$$\tau_{out} = \tau_{in}\sqrt{1 + \frac{16(\ln 2)^2 GDD^2}{\tau_{in}^4}}$$

TPA-TCT at CERN

2016: Presentation of TPA-TCT at CERN to CERN KT Fund Selection Committee
→ Funding to build a compact TPA-TCT setup at CERN SSD lab

2nd of July 2019: First TPA-TCT signal at CERN

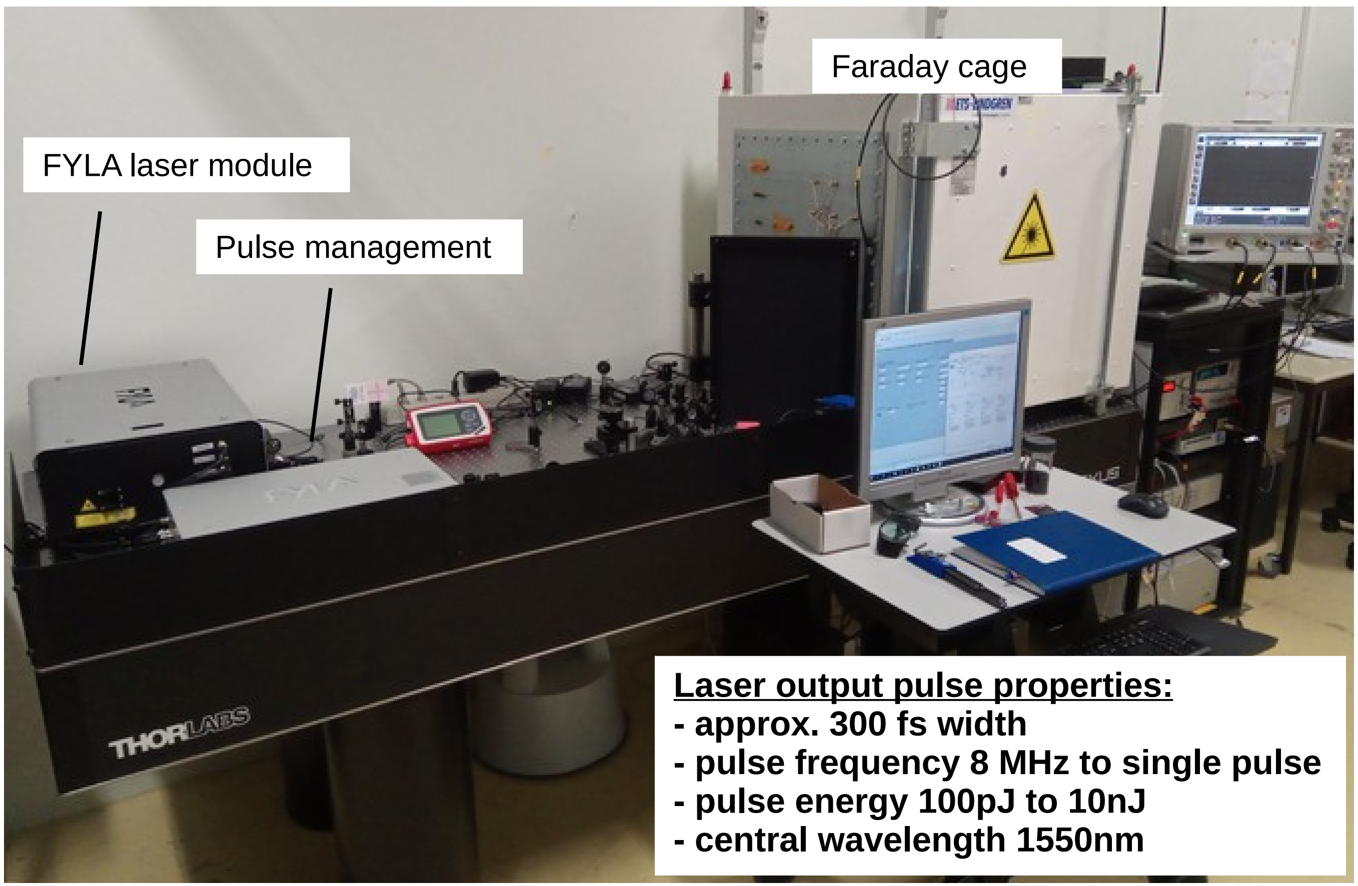

Laser output pulse properties:
- approx. 300 fs width
- pulse frequency 8 MHz to single pulse
- pulse energy 100pJ to 10nJ
- central wavelength 1550nm

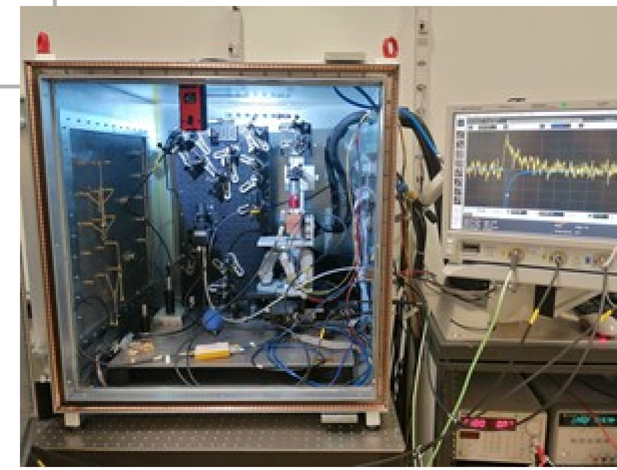

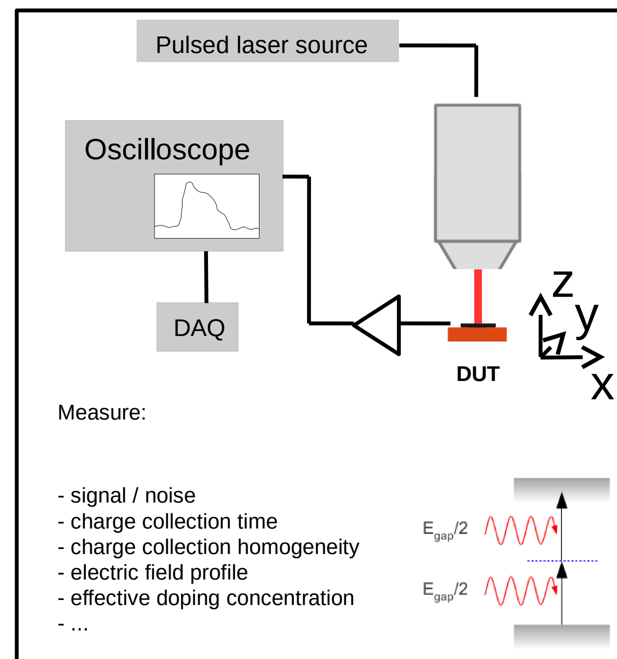

M. Wiehe, "Development of a Tabletop Setup for the Transient Current Technique Using Two-Photon Absorption in Silicon Particle Detectors,"
IEEE Transactions on Nuclear Science, vol. 68, no. 2, pp. 220-228, Feb. 2021
https://doi.org/10.1109/TNS.2020.3044489

Pulse Management

- **Acousto-optic-modulator** for selecting the pulse frequency: 8.1MHz to single shot
- **NDF**: Motorized ND-filter, variable pulse energy 0-10nJ (at laser output)
- **Electrical trigger**: InGaAs detector used for triggering (before power adjustment)
- **SPA reference**: InGaAs detector for power monitoring

Pulse Management Module

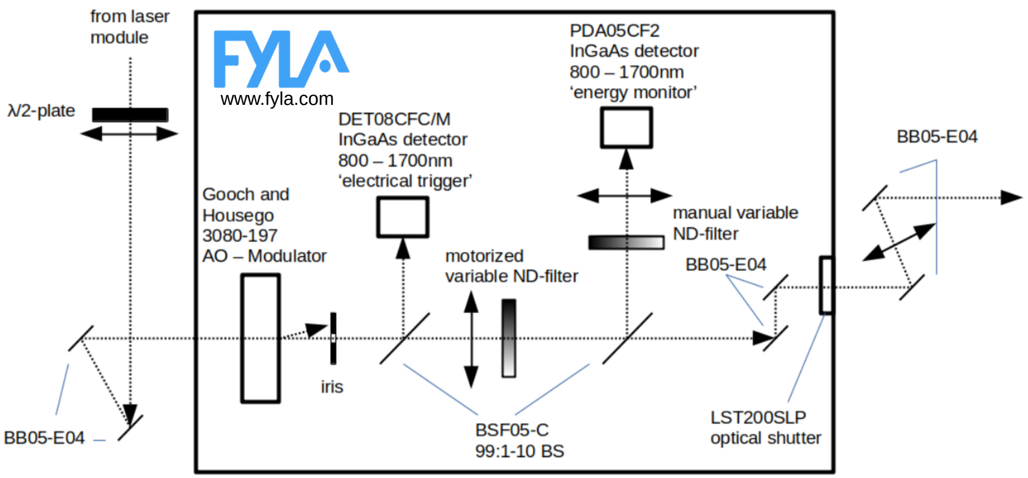

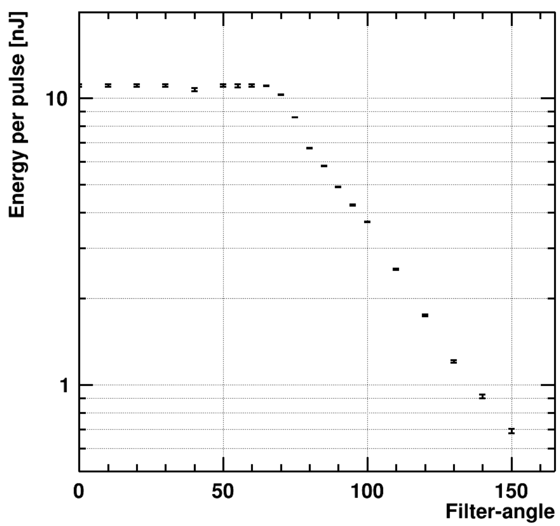

TPA-TCT at CERN

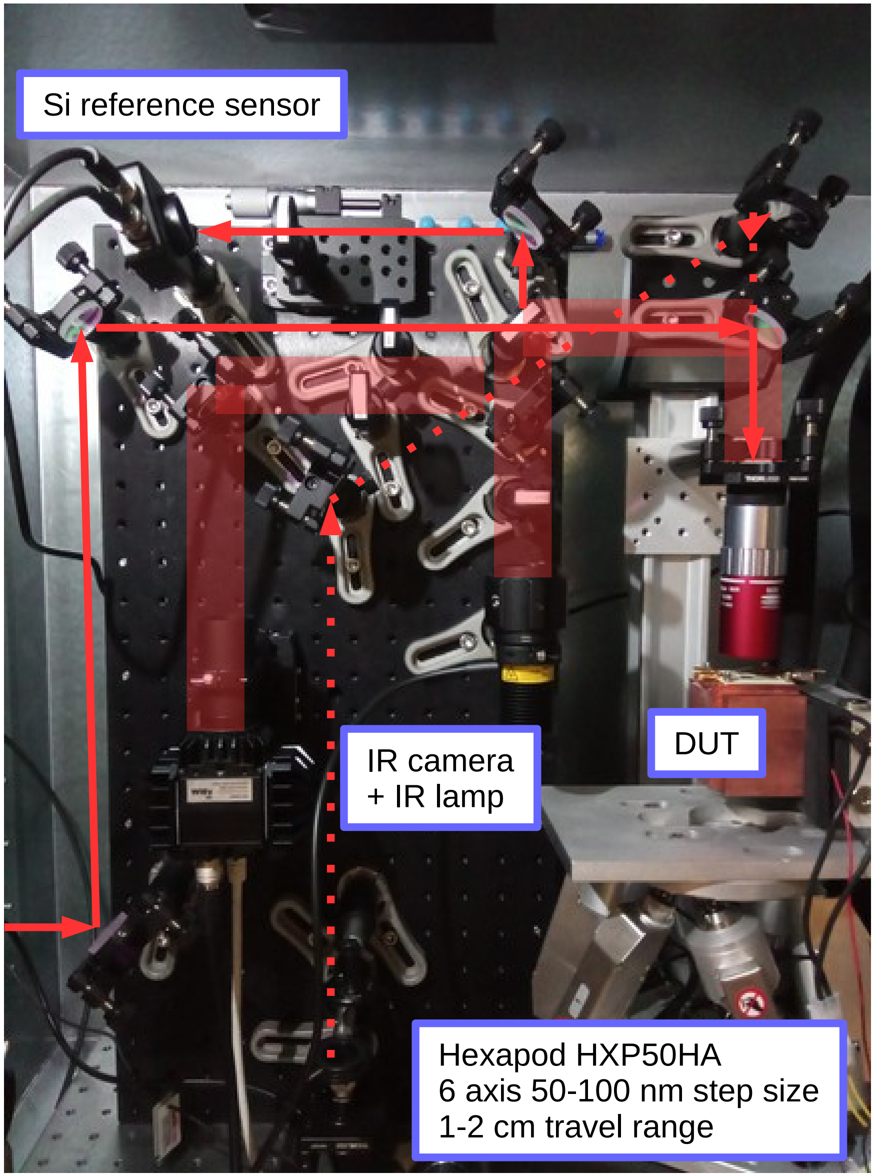

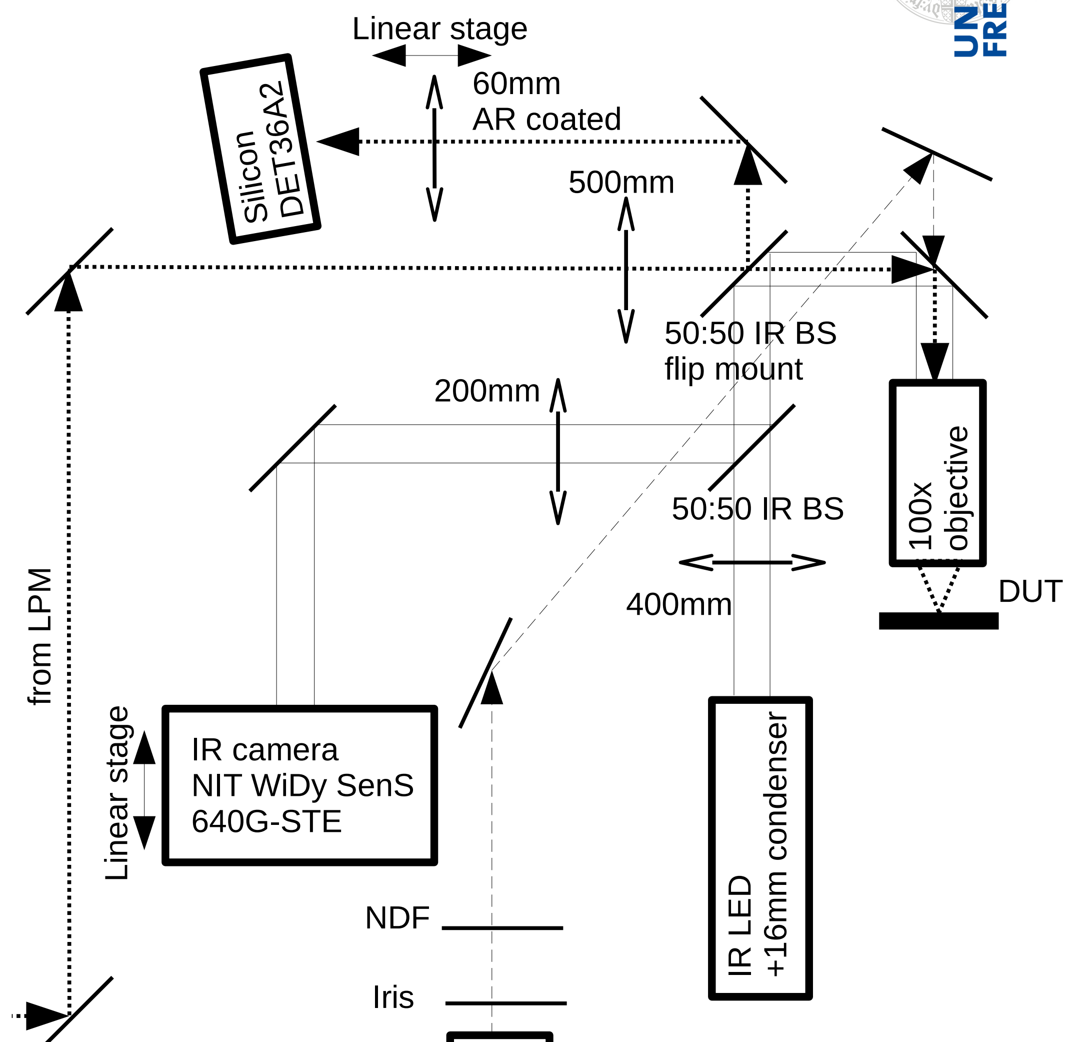

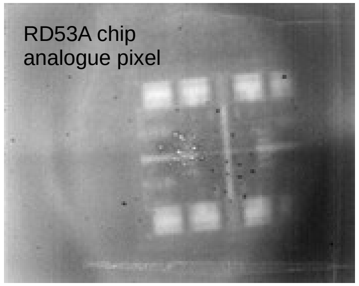

Power and Charge

The laser power is adjusted with a neutral density filter (NDF) inside the pulse management module.

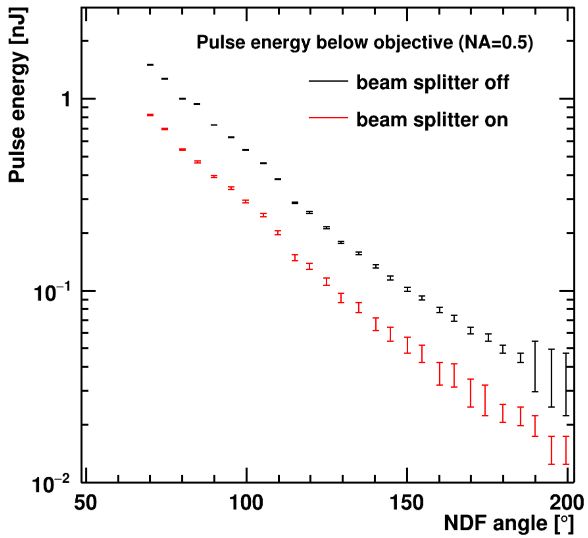

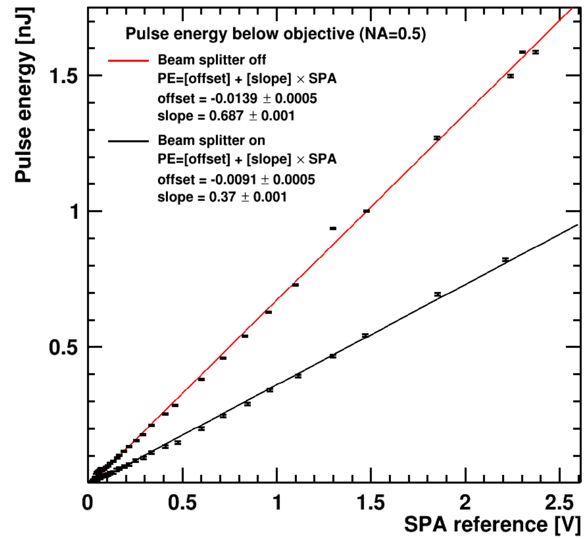

Measurement of the laser power below the objective (position of DUT)

- Power meter PMD100D+S401C (thermopile)
- Pulse frequency=4.051MHz
- T=23°C

Variable pulse energy 0-10nJ (at laser output) reduced to 1nJ below objective

2nd order absorption (TPA)
→ quadratic dependence of signal on laser power

$$\frac{dN(r,z)}{dt} = \frac{\alpha I(r,z)}{\hbar\omega} + \boxed{\frac{\beta_2 I^2(r,z)}{2\hbar\omega}}$$

Carrier Generation equation

(1MIP in 300µm ~ 3.6fC)

NA = 0.5

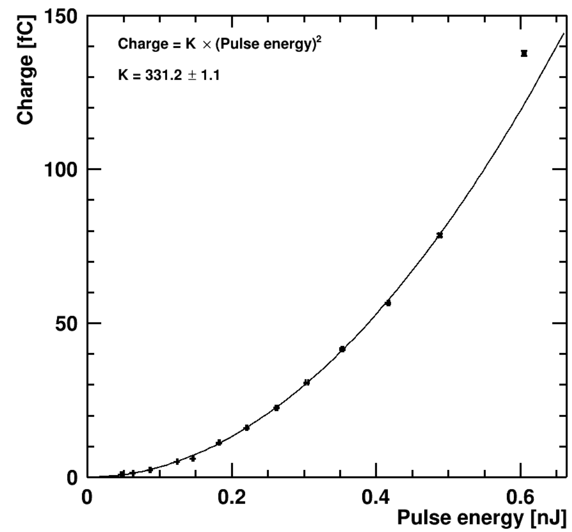

Measurement of the collected charge inside a silicon sensor (7859-WL-A63-PIN4) with a charge sensitive amplifier

- CxL0058, Diamond Spectroscopic Amplifier
- Gain=12.5 mV/fC

50:50 beamsplitter for TPA reference and IR camera in place.
Can be removed after alignment.

- 2x energy
- 4x charge
- no TPA ref, no IR camera

Reflection not taken into account: 30% light reflected on silicon surface

Power correction

A reference signal is used to correct the DUT-signal for fluctuations in the laser power

First tests with an SPA reference failed:

- Fluctuations in laser power (affect SPA + TPA)
- Fluctuations in pulse temporal profile (affect only TPA)

→ **Reference the DUT against a TPA-signal to correct for instabilities**

Work in progress: Increase reference amplitude to increase SNR

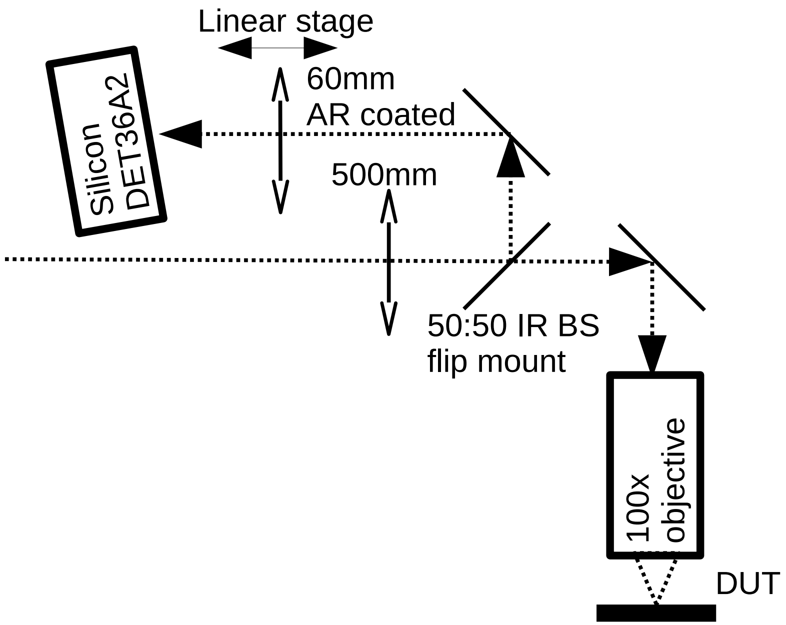

SPA reference

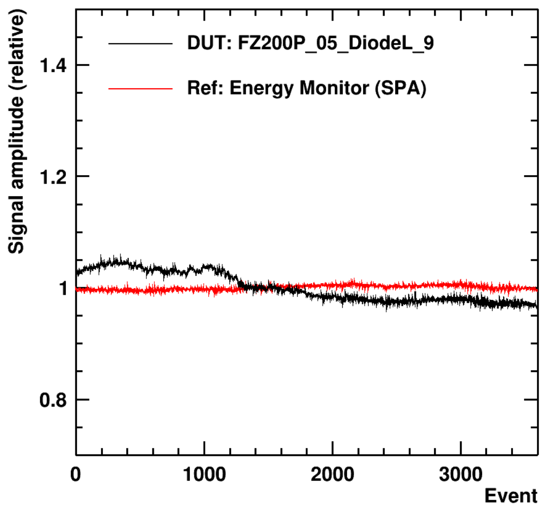

TPA reference

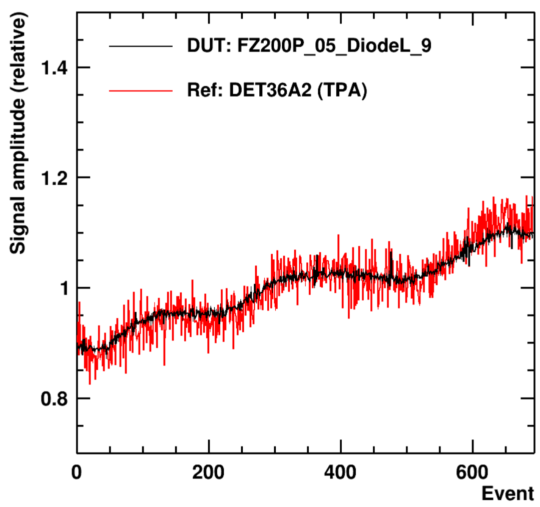

Second Harmonic Generation

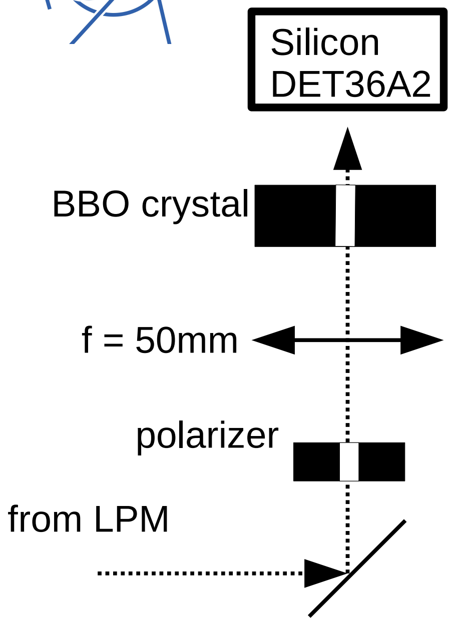

(polarizer only to check incident polarization, it doesn't do anything..)

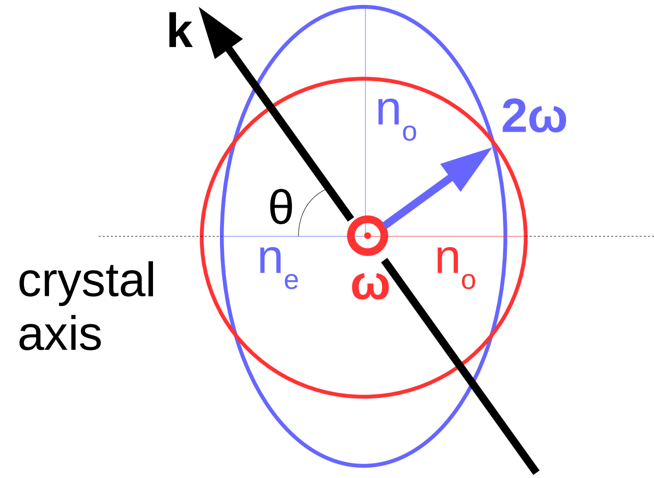

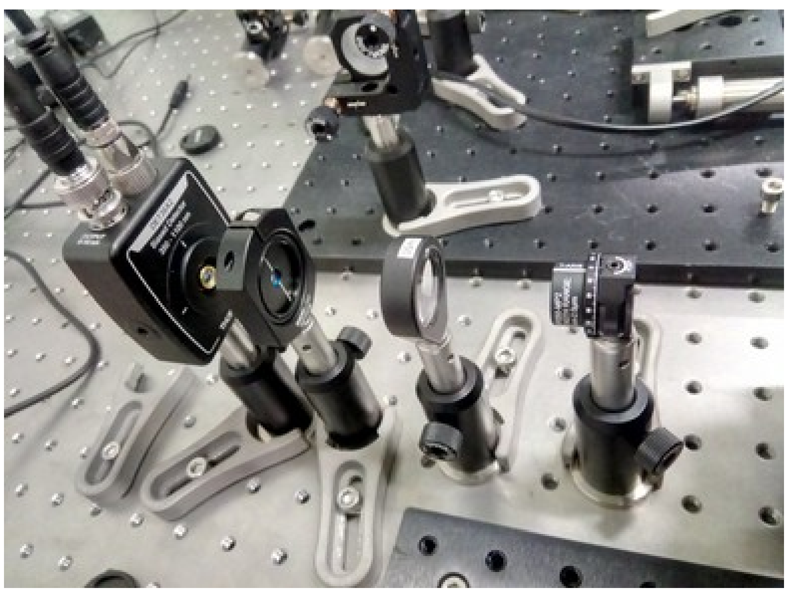

White mark on the crystal housing is perpendicular to the crystal (extraordinary) axis.
→ needs to be parallel to polarization of incident beam

Crystal is cut with θ=20° angle, so that beam enters with normal incidence.

SHG was tested as a method to obtain a reference signal.

Discarded because..

- the signal amplitude is very low
- very sensitive to alignment
- sensitive to temperature changes

- but: could in principle be set up without sacrificing a part of the beam

Knife-edge scan

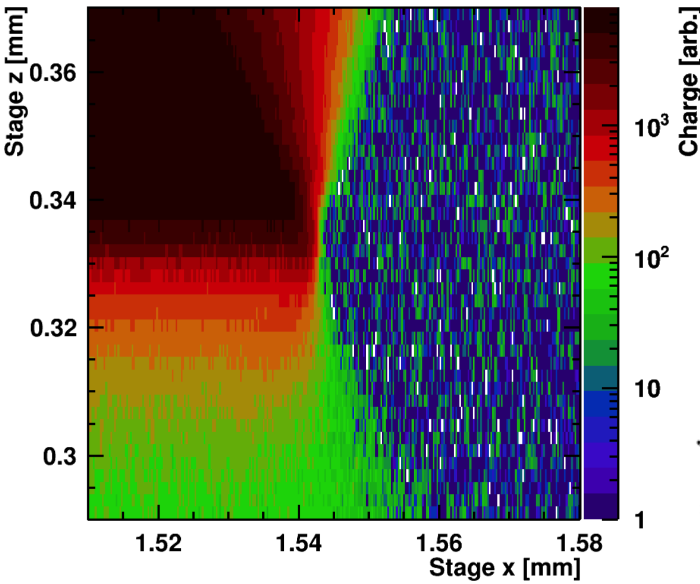

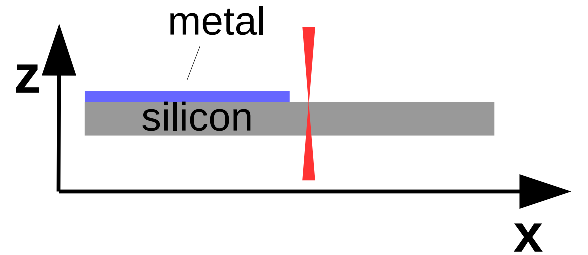

Fit Q(x) for every z with

$$\int_{-\infty}^{x}\int_{-\infty}^{\infty} n_{tpa}(x',y,z)\,dy\,dx' = \frac{E_p^2\,\beta_2\lambda\ln 2}{4\sqrt{\ln 4}\,c\,\hbar\,\pi^{\frac{5}{2}}\,\tau\,w^2(z)}\left[1+\mathrm{erf}\left(\frac{2x}{w(z)}\right)\right]$$

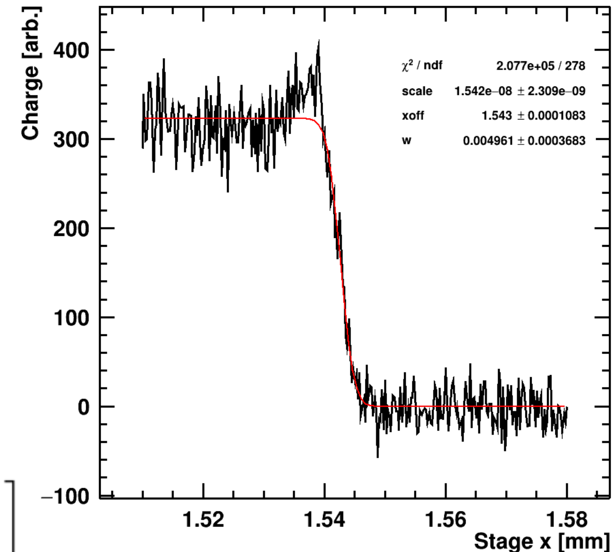

For every z, an erf() is fitted to Q(x) to obtain the beam radius w(z).
w(z) can be fitted to obtain the waist radius w0 and Rayleigh-length z0.

Z-values need to be corrected/scaled due to the effect of refraction:

$$z' = z\cdot\sqrt{\frac{z_0\,\pi n^3}{z_0\pi n-\lambda n^2+\lambda}}$$

Shape of the focal point in silicon
Rayleigh length z_0=12.5µm
2σ radius at the beam waist w_0=1.4µm

z_0 = 12.5µm, w_0=1.4µm

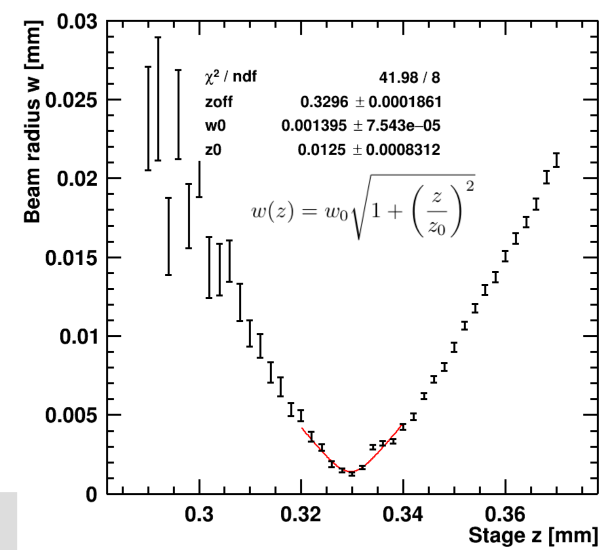

More results (NA=0.7) in the next talk
Sebastian Pape – TPA-TCT: Results

Resolution along beam direction

<u>SPA</u>: Light absorption anywhere along beam

<u>TPA</u>: No signal, if focal point not inside detector

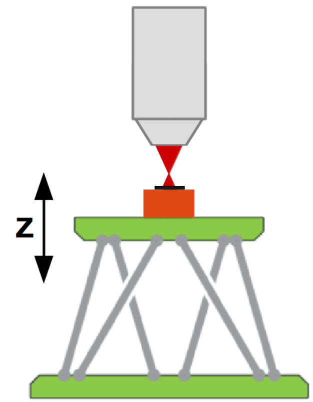

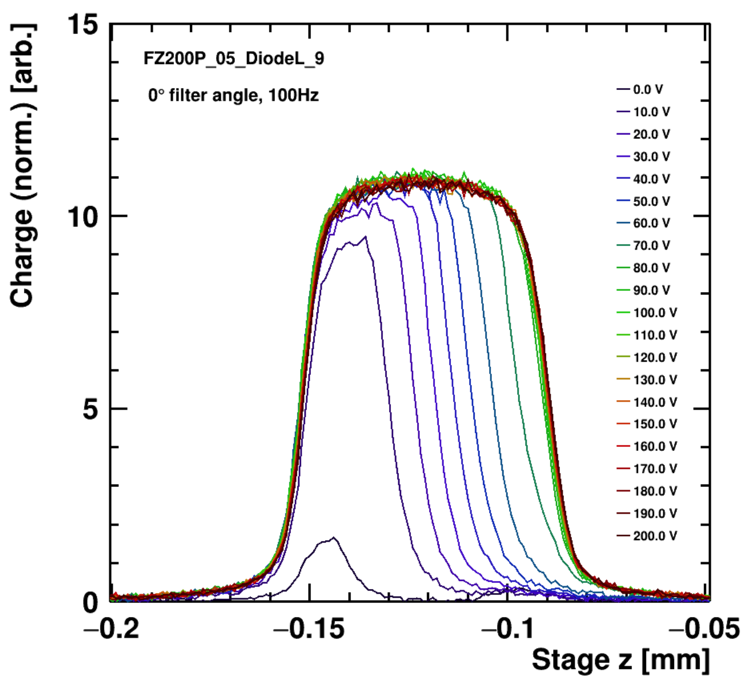

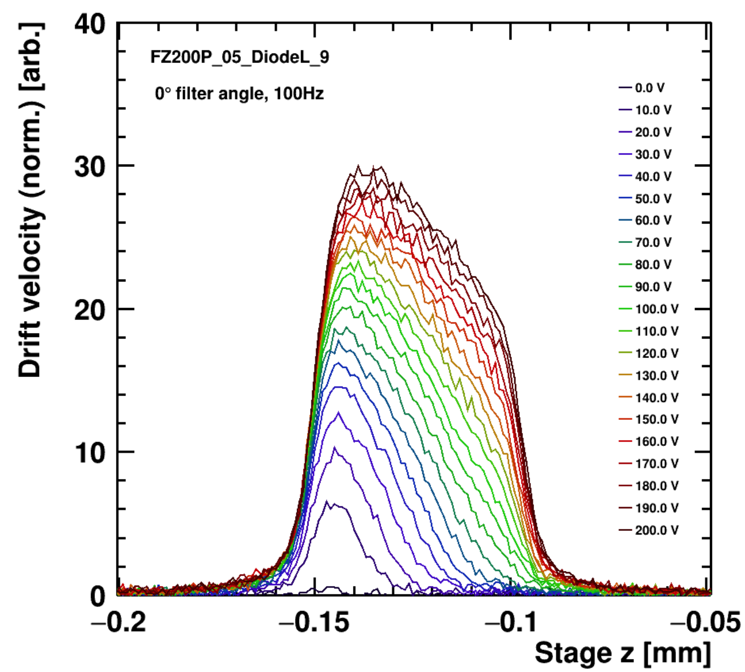

Note: Measurements for a given (x,y)-position on the sensor

More results in the next talk
Sebastian Pape – TPA-TCT: Results

Hexapod: Tilt correction

- Drift velocity dependence on x,y position measured → sensor is tilted
- Four z-scans at different positions → obtain sensor surface at rising edge of Q(z)
- Plot sensor surface, z against x,y
- Fit to obtain angles wrt. coordinate axes

Fit plane to surface: $z = z_0 + a_x x + a_y y$

angles in xz- (yz)-plane of x- (y-) axis to sensor

$$\alpha = \arctan(a_x) \text{ and } \beta = \arctan(a_y)$$

- Move hexapod carriage by angles

$$u = -\beta \text{ and } v = \alpha$$

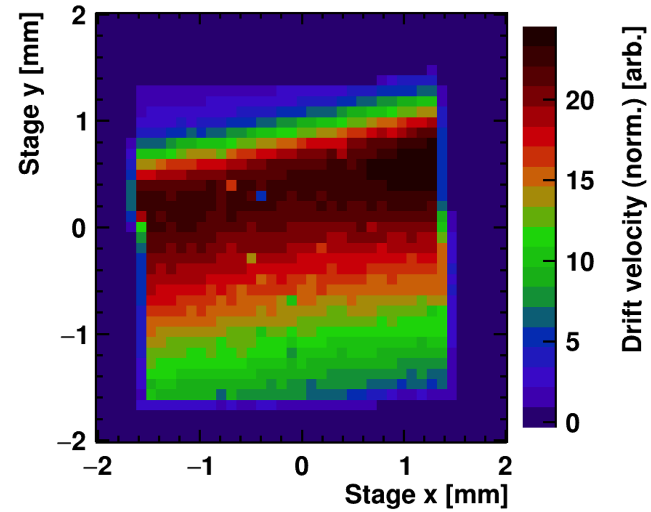

Hexapod HXP50HA
6 axis 50-100 nm step size
1-2 cm travel range

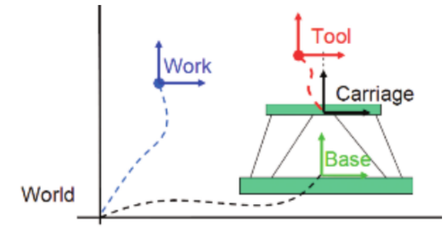

4x

angle to x axis α= -0.1745°
angle to y axis β= 1.1278°

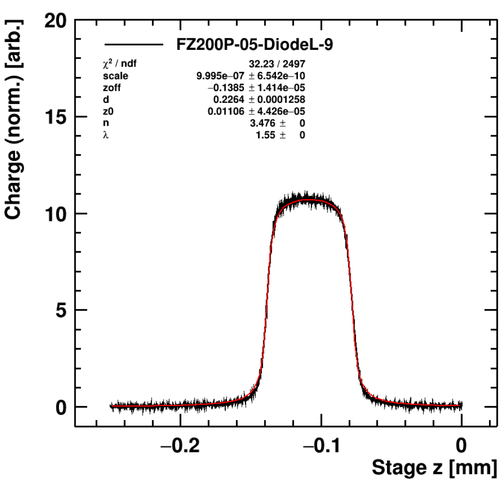

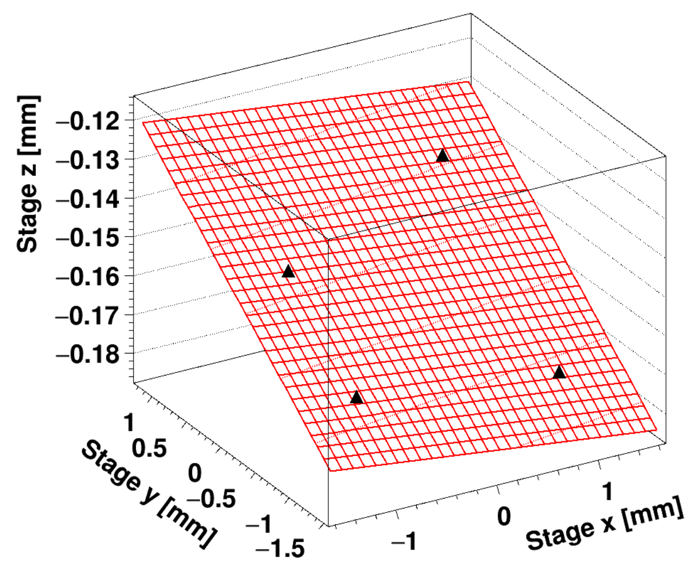

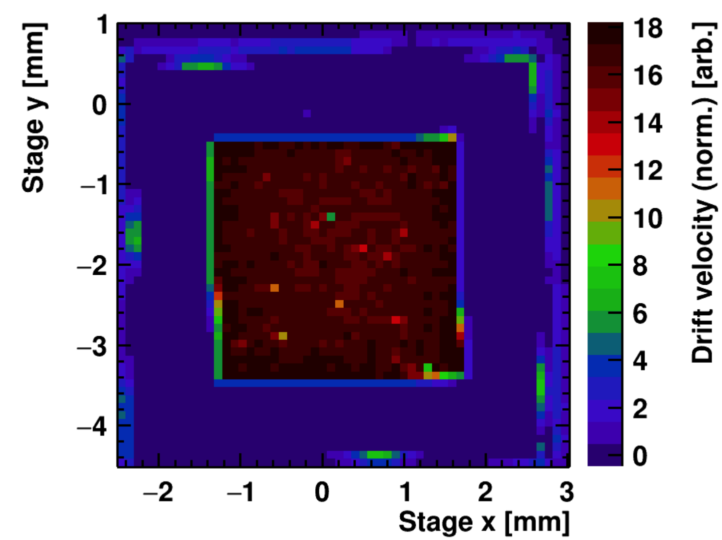

Note: An angle of 0.1° over 3mm corresponds to 5µm height difference.

Rotation of the coordinate system

The hexapod has a limited angular range of several degree..
To be able to scan along certain axes, if the DUT is not mounted parallel to the coordinate axes, the work coordinate system can be redefined:

Here a redefinition of the work system of w=-20° was applied.
This is not a physical rotation of the stage.
The negative angle rotates the coordinate system clock-wise.

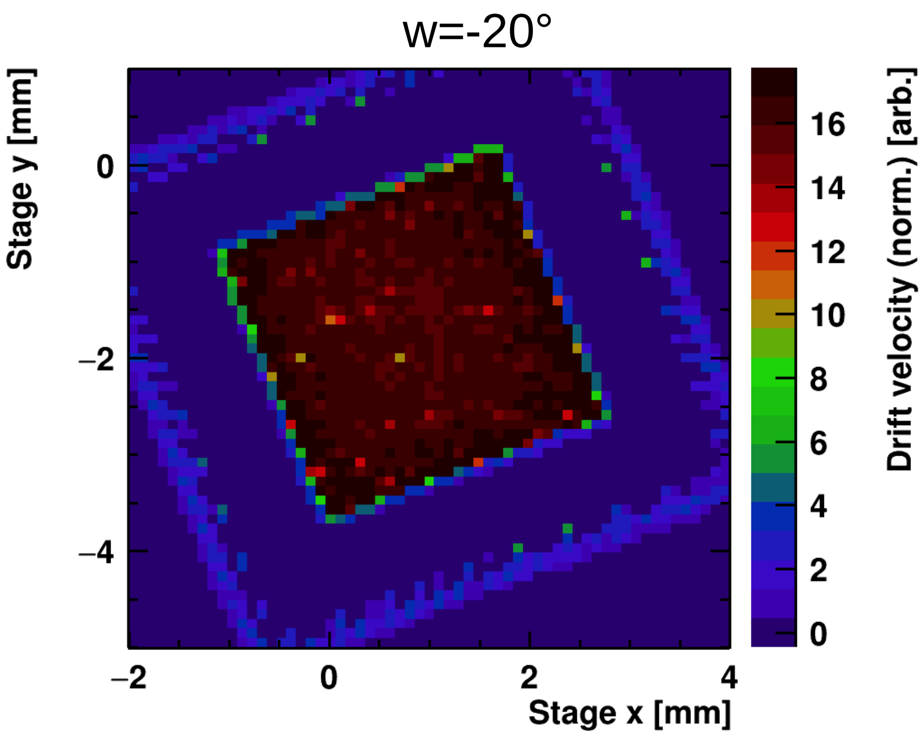

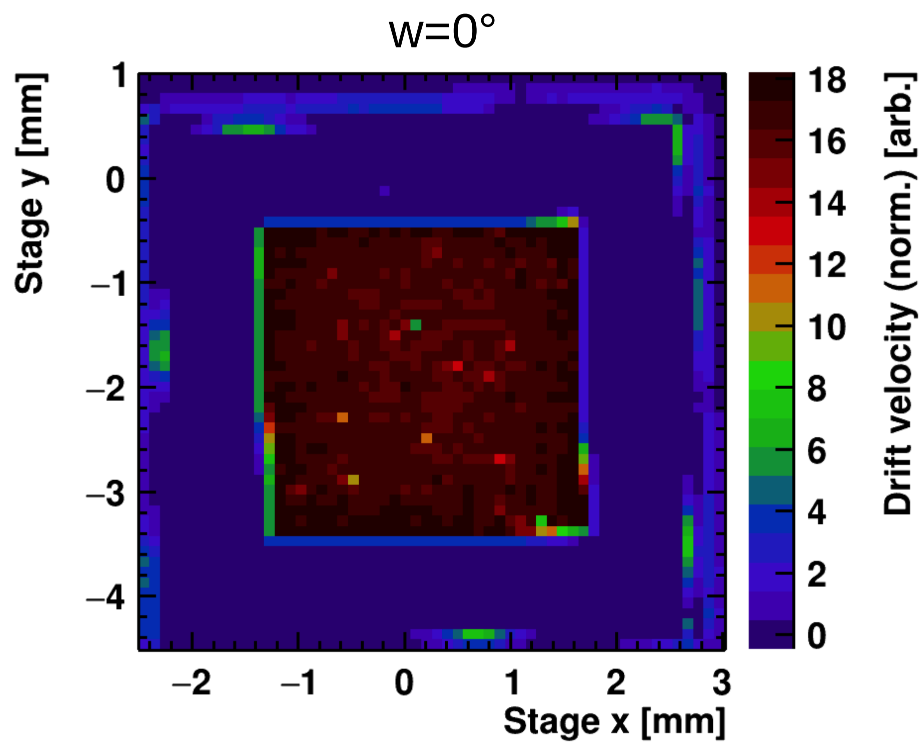

Conclusions

The method of TPA-TCT was tested at UPV/EHU and presented to RD50 in 2015.

A compact TPA-TCT setup was developed at CERN.

- Variable pulse energy 0 – 10nJ at the laser output, 0 – 1nJ at the DUT
  Charge generation 0 – 200fC with NA=0.5
- 3D resolution with NA=0.5: z0=12.5µm, w0=1.4µm
  NA=0.7: z0 = 6µm, w0=0.9µm (see next talk)
- Correction of power/spectral fluctuations by a TPA or SHG reference is crucial.
- Precise positioning of the sample and correction of angular misalignment (Θ ~ 0.1°) is important.

Temperature dependence of collected charge in TPA-TCT

- Measurement of the charge at different temperatures [-20°C;+20°C] with different laser powers (NDF angles)
- Sensor: 7859-WL-A63-PIN4, 100V, Charge sensitive amplifier CxL0058, tilt corrected, not irradiated, physically ~285 µm thick, no support wafer
- Laser freq: 200Hz

Higher absorption at higher temperatures expected:
- The band gap decreases with higher temperature
- Band-to-band absorption in Si is indirect (phonon assisted)

- Fit with linear function, [p0] = fC, [p1] = fC/°C
  Normalize slope by charge at 0° (~ mean, result depends slightly on temperature: 0.0067 (-20°C) to 0.0053 (+20°C))
  Normalized Temp.C.=p1/p0, [1/°C]
- Weighted average: Normalized Temp.C.= (0.0059 +/- 0.0004) 1/°C

- E.g.: at 100fC a temperature change of 40°C leads to a difference of $0.0059°C^{-1}$ x 100fC x 40°C = 24 fC

Q = p0 + p1 x T

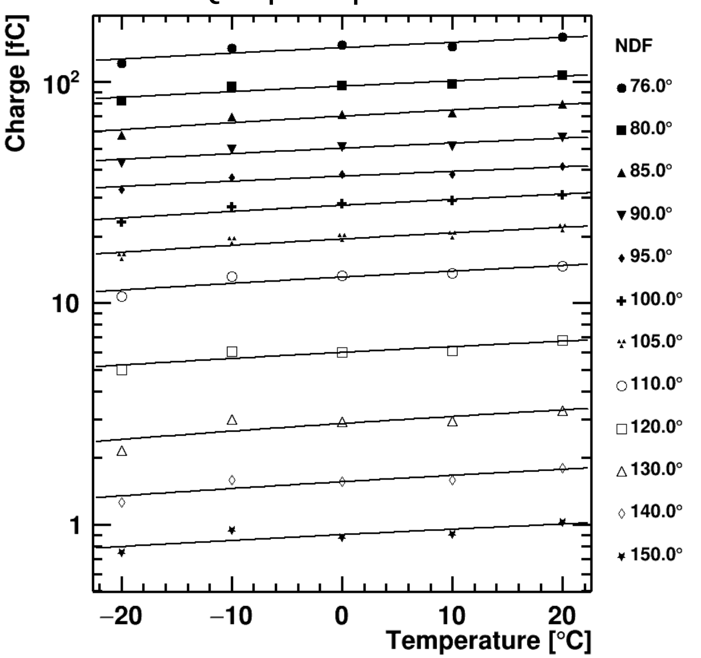

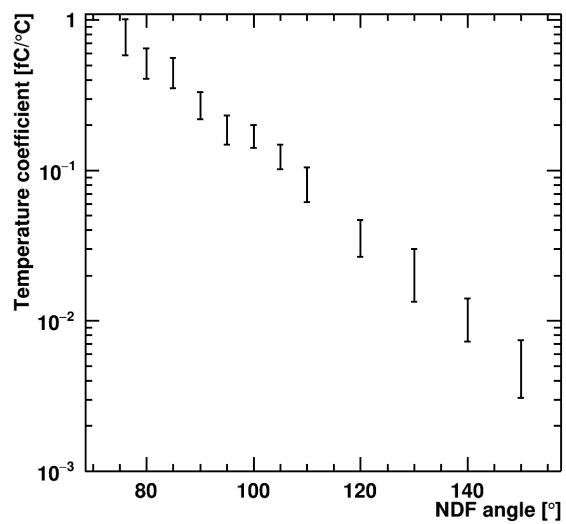

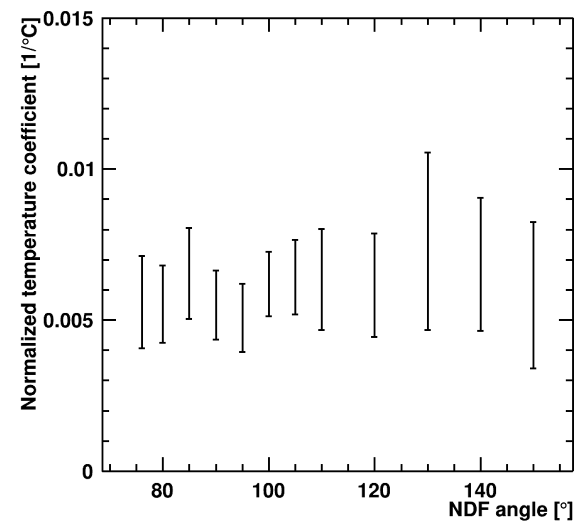

Inter-pad region: HPK2-LGAD

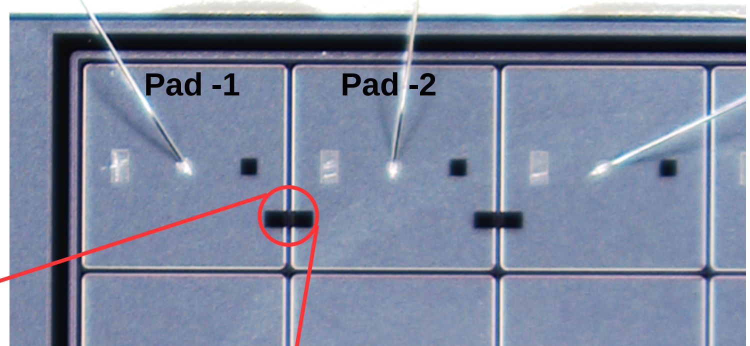

HPK2-W28-S1-LGAD-P14
LG 5x5-SE3-IP5-UBM

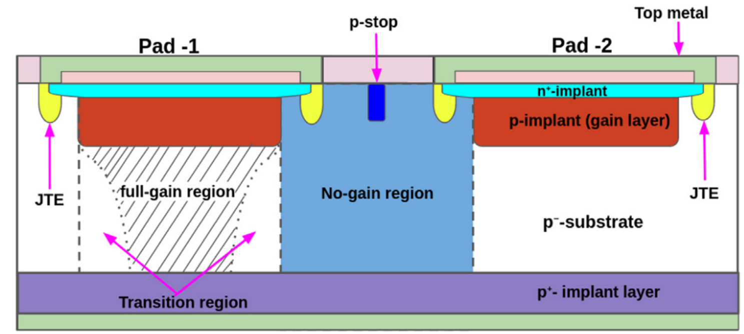

S. Bharthuar et.al.
https://doi.org/10.1016/j.nima.2020.164494

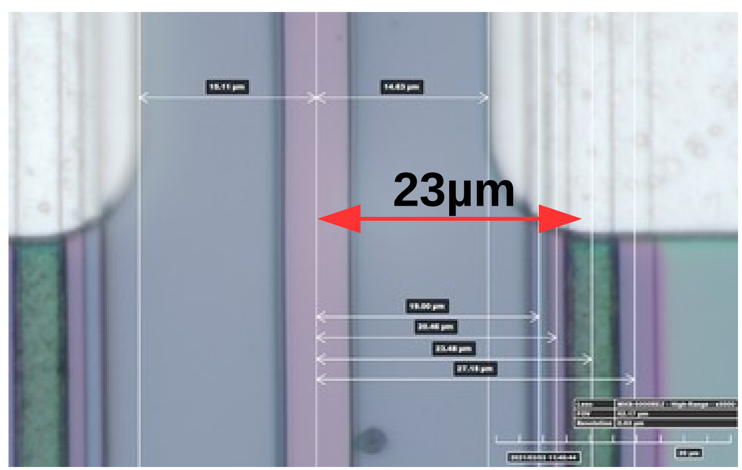

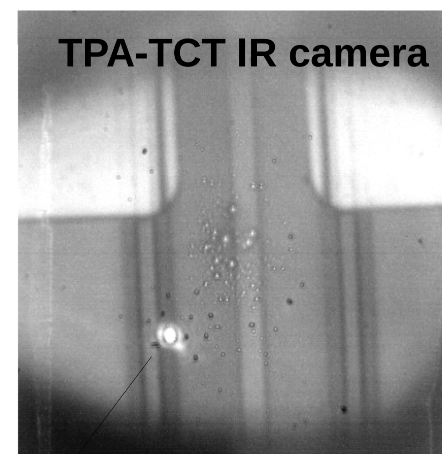

laser beam spot

Images with Hirox microscope
CERN EP-DT QART lab

Inter-pad region: HPK2-LGAD

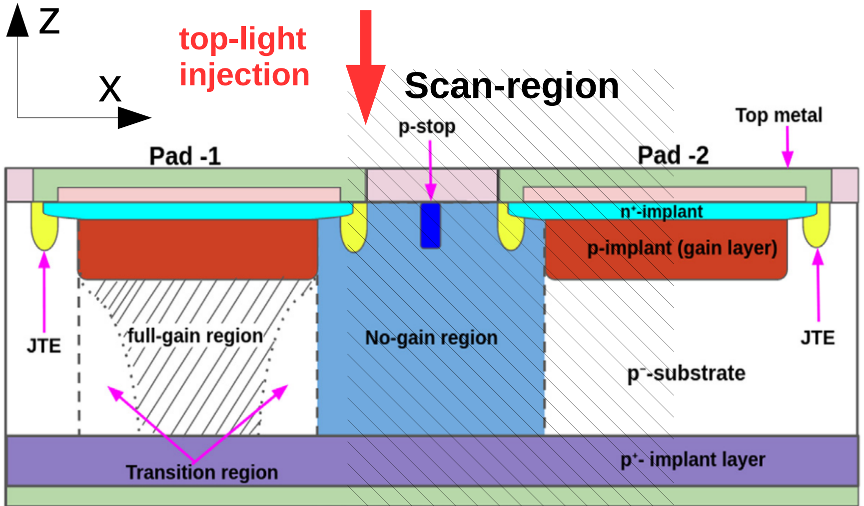

S. Bharthuar et.al.
https://doi.org/10.1016/j.nima.2020.164494

(not to scale)

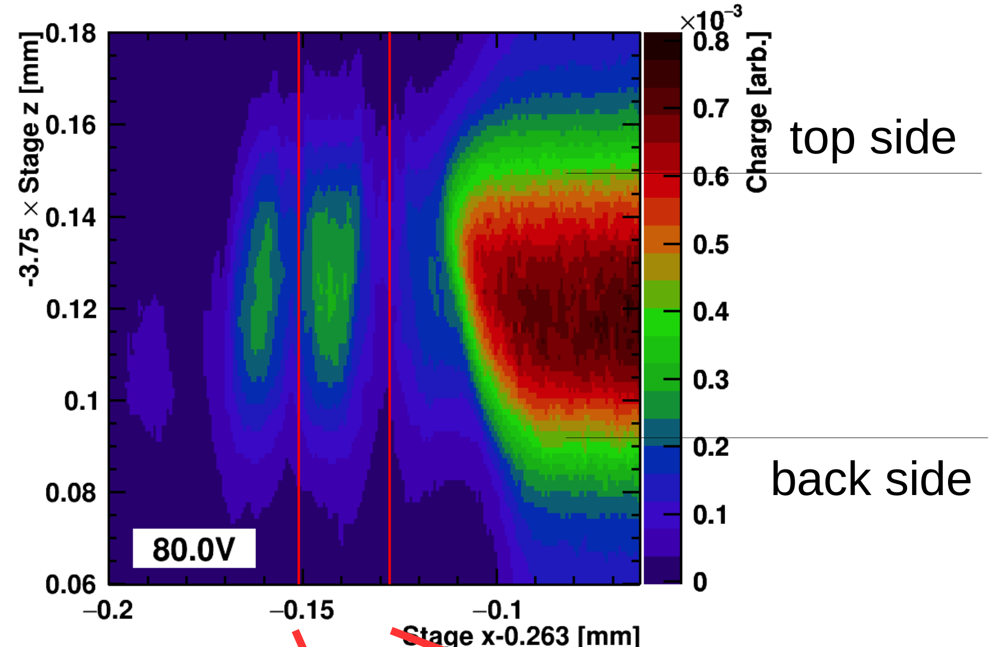

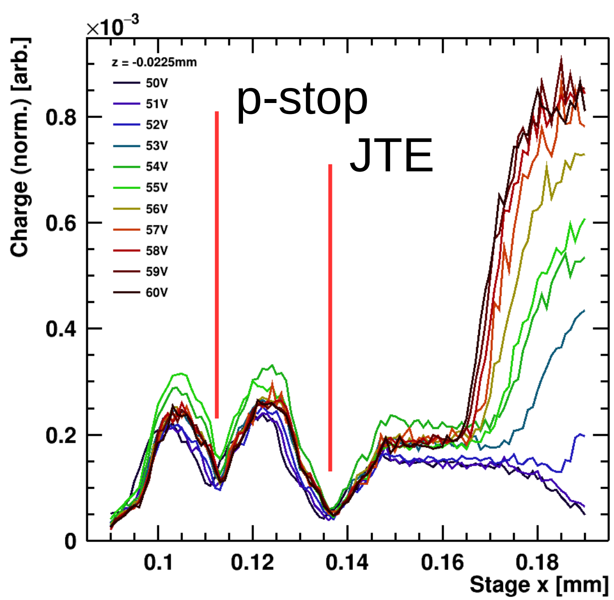

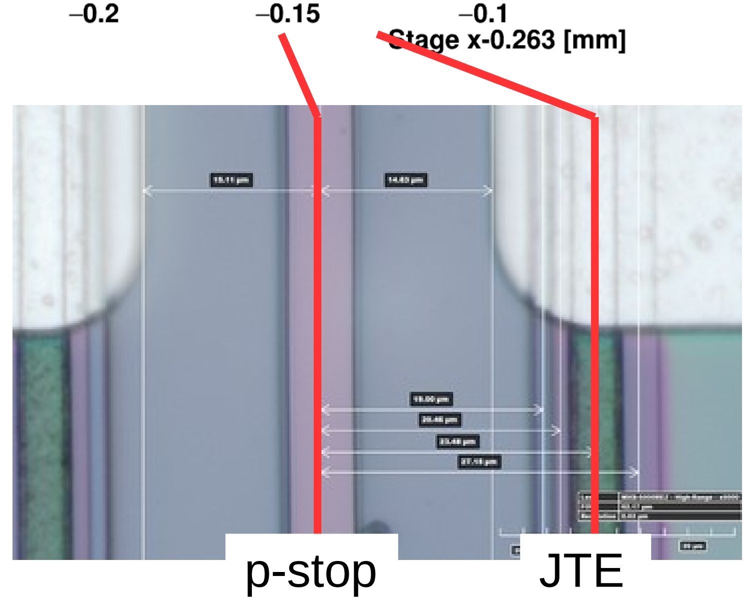

HV-CMOS

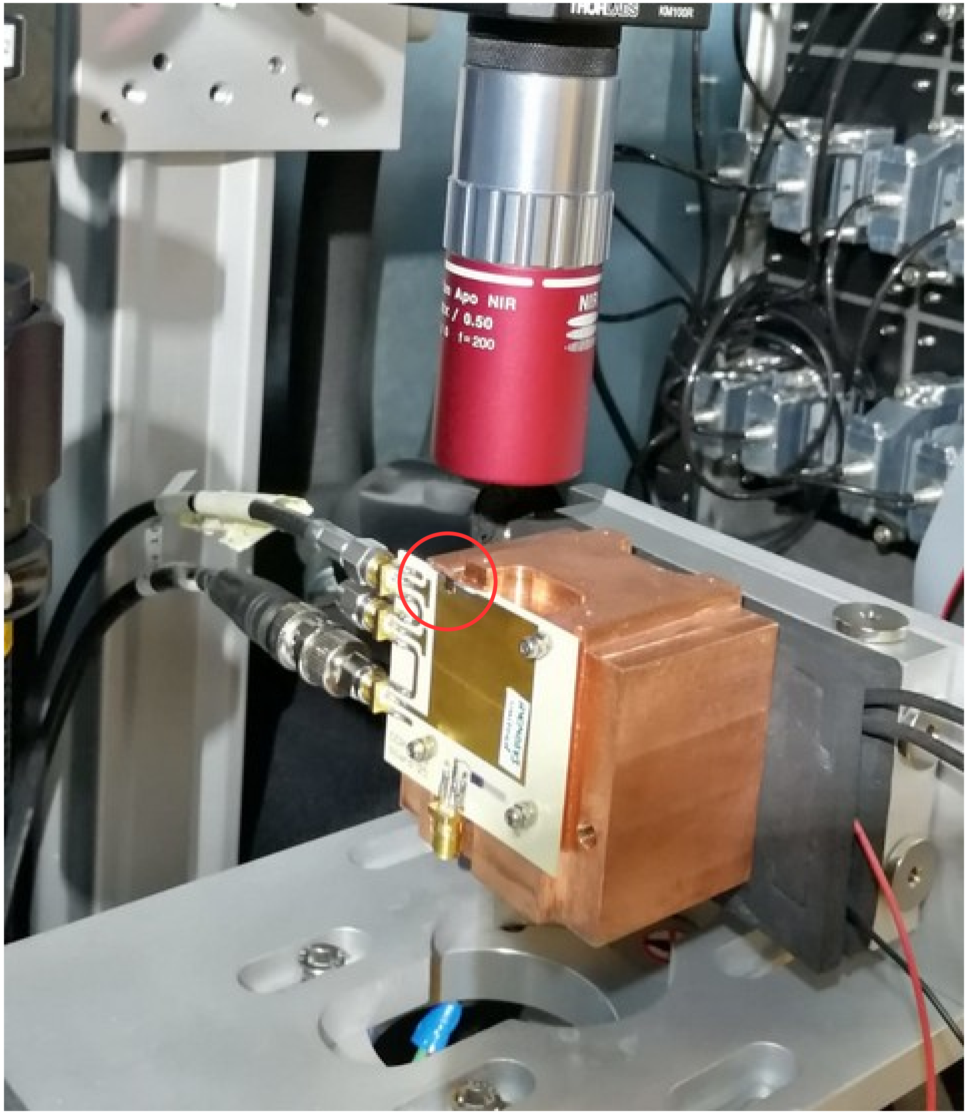

Finding the device and the active volume under the objective is challenging.

The active volume has a size of approx. 120 × 25 µm and is buried 50µm deep under the surface (in the direction of the beam).

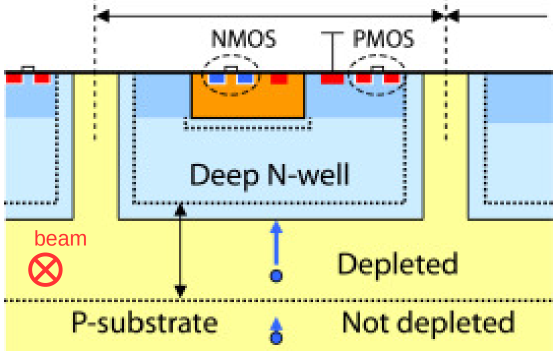

https://doi.org/10.1016/j.nima.2016.06.001

HV-CMOS

Three signal regions are identified.
Implant, low amplitude, slower signals
Drift region, high amplitude, fast signals
Diffusion region, very long signals, charge carriers diffuse into depleted region

charge integration time 25ns

drift velocity integrated 600ps
same distribution for lower
integration times (100-600ps)

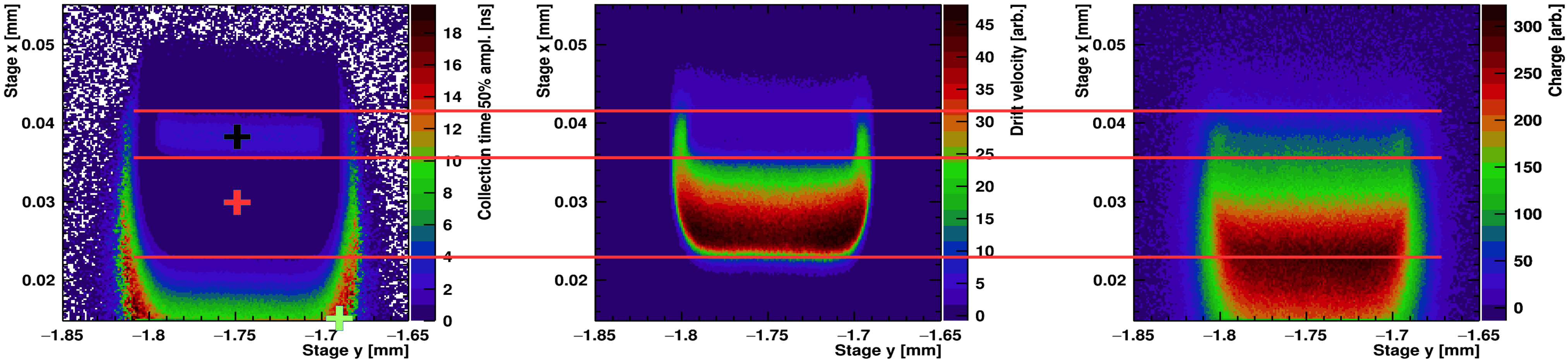

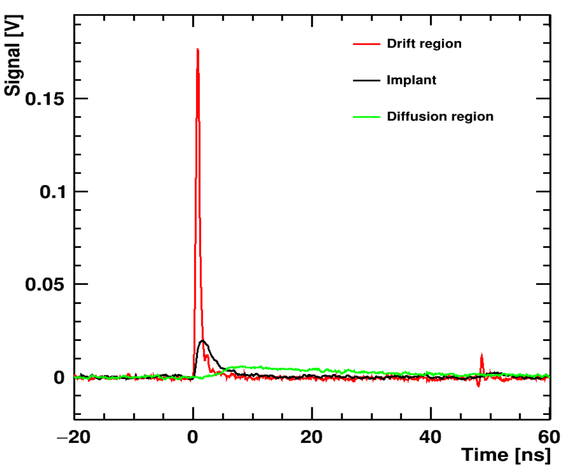

DNW can not be identified in collected charge.

Focal point is ~50µm below the surface.
Gradient of collected charge (and drift velocity) likely due to clipped beam.

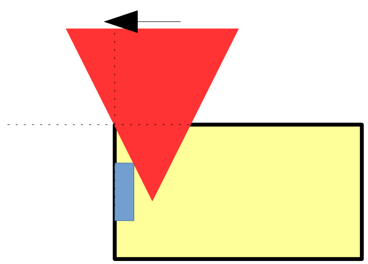

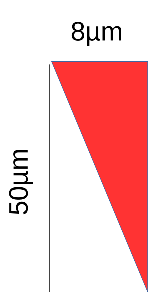

NA=n·sin(θ)

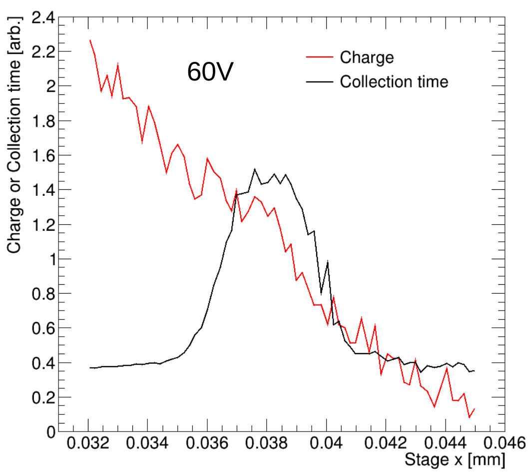

Strip Detector

Micron strip detector: FZP2328-11

- **p-type, 80µm pitch, 30µm strip metalization width**
- **300µm thickness**
- **non-irradiated**
- **Central strip bonded, 2 neighbors bonded**
- **backside bias**

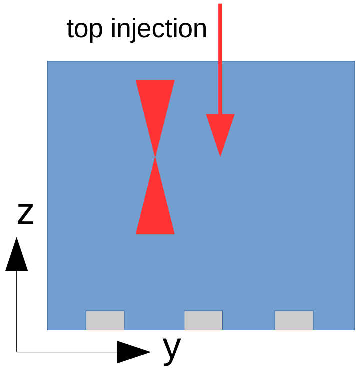

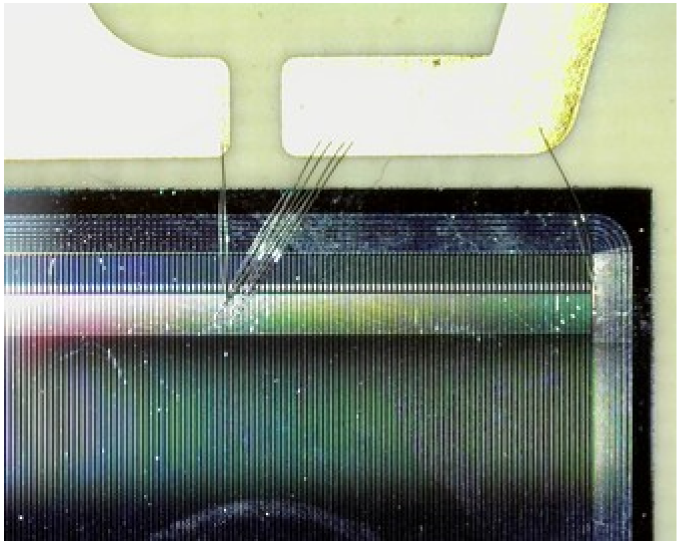

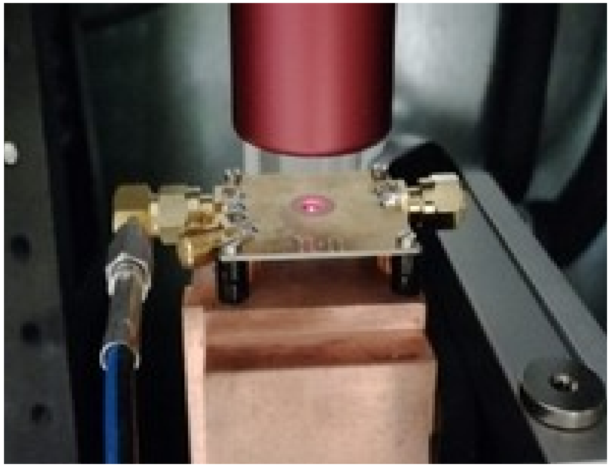

back illumination

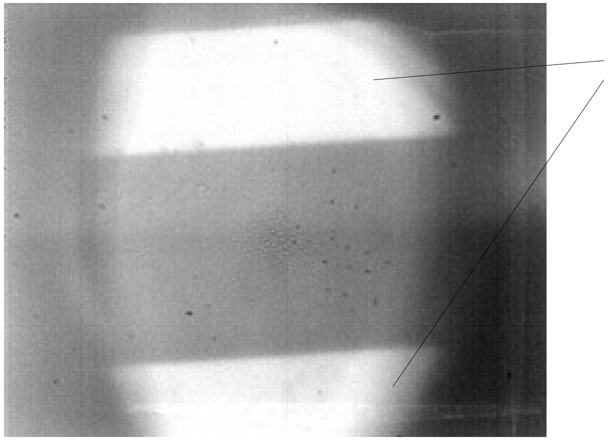

strip metalization

Strip Detector

reflection on metalization increases irradiance and $Q \sim I^2$

contour lines at Q=0
negative charge
- cross-talk
- ballistic deficit

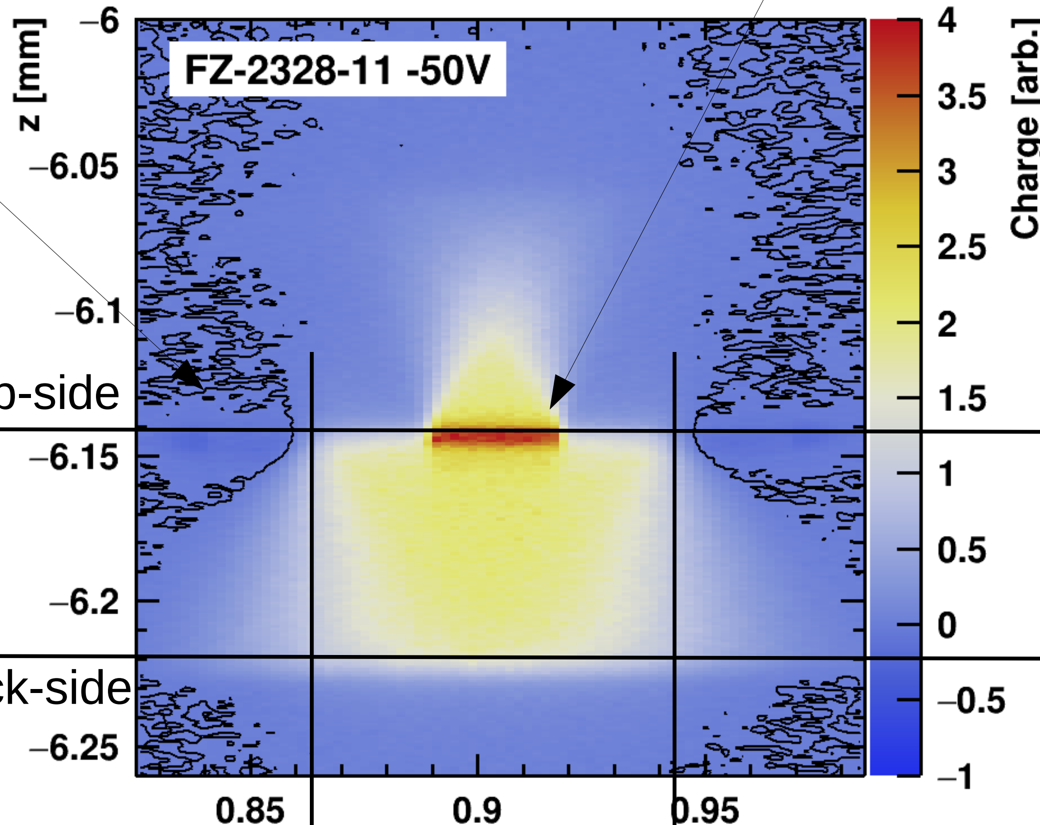

sensor top-side

80µm measured refraction!
80 x 3.75 = 300µm

sensor back-side

80µm pitch

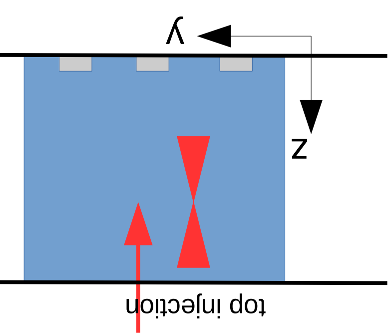

Strip Detector

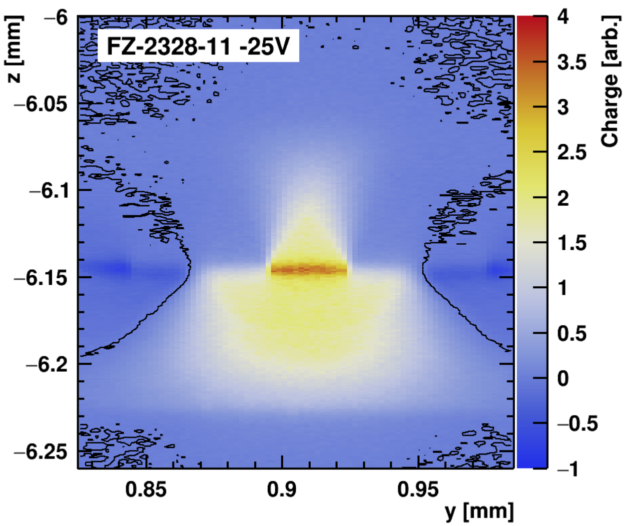

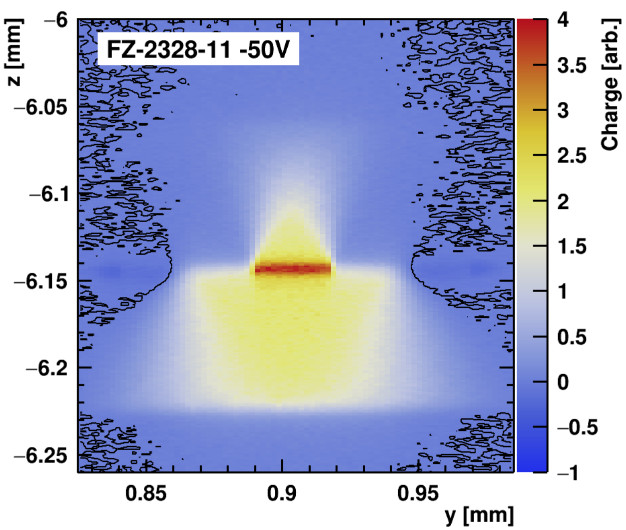

- Reflection on metal leads to increased irradiance → higher charge ($Q \sim I^2$)
- Light is also reflected on Si-air interface but does not lead to a pronounced peak
- Slope of collected charge between strips due to charge sharing

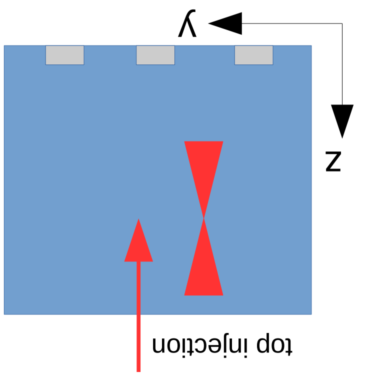

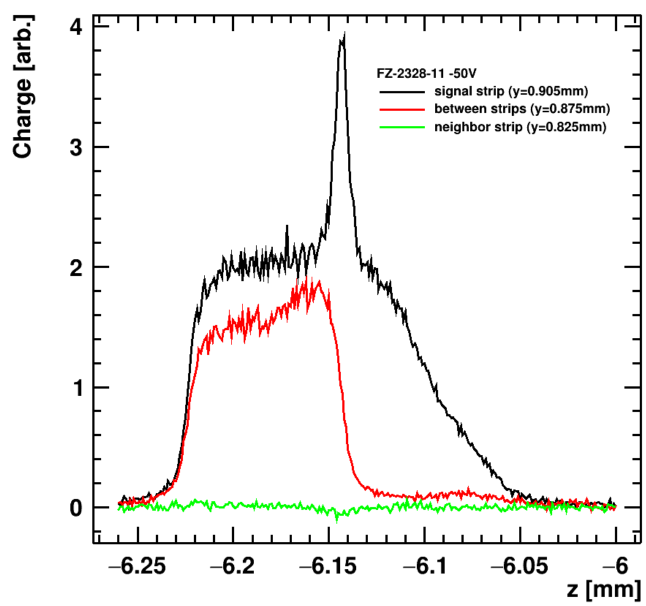

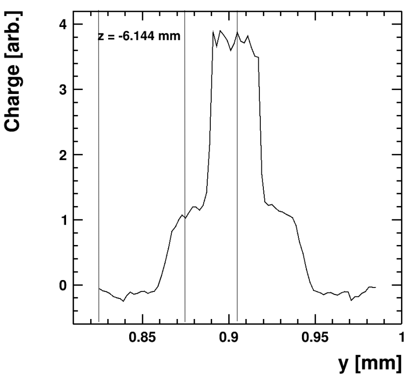

symmetric pulse shape vs. z

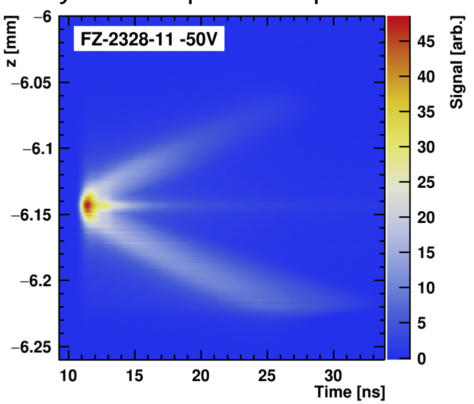

Reflections on Si-Air interface

Fresnel equation for normal incidence

$$R_0 = \left| \frac{n_1 - n_2}{n_1 + n_2} \right|^2$$

~30% for Si – air
→ 10% of charge expected ($Q \sim I^2$)

Light is reflected on the backside of the detector, leading to a mirror image.
Symmetry can be observed e.g. in charge / drift velocity / signal shape.
Reflection depends on backside processing:

- No reflection for deep diffused with support wafer
- Mirror-image with ~10% amplitude on Si – air interface
- Strong reflection with pronounced peak at metal layer (strip or back side metalization)

7859-WL-A63-PIN4
Not irradiated
Physically ~285 µm thick
No support wafer

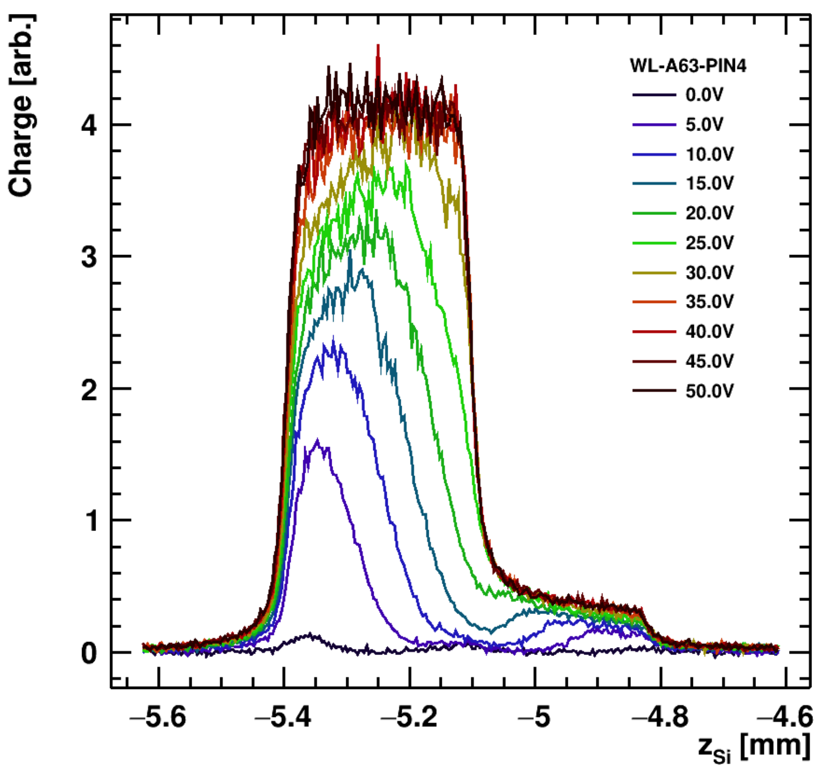

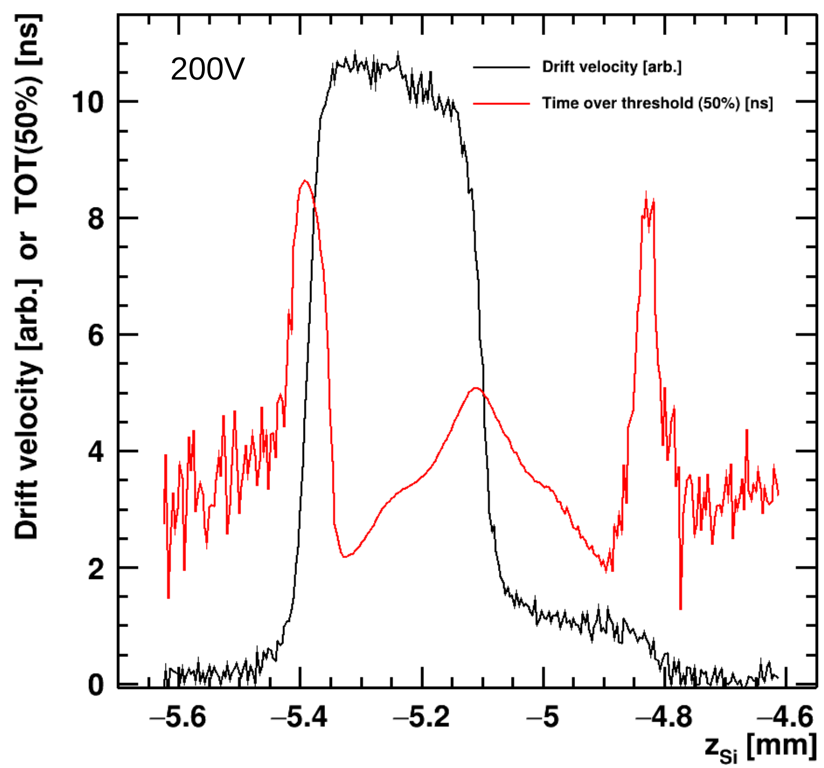

Irradiated Detectors

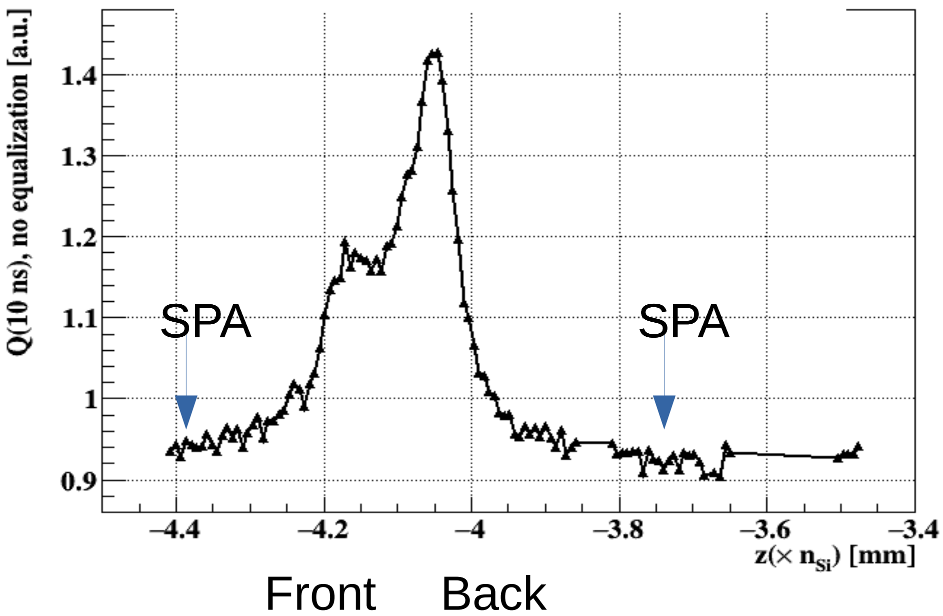

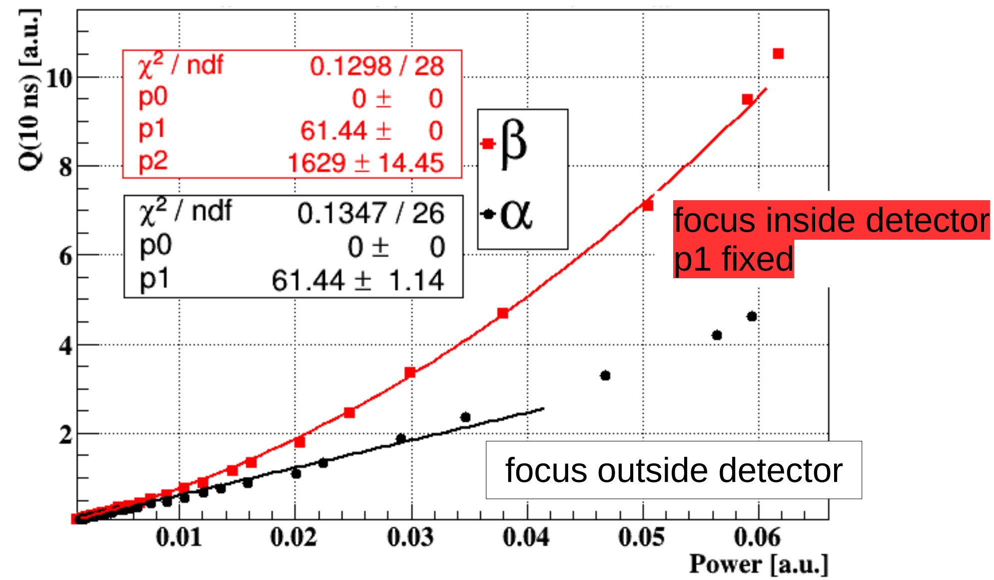

- Irradiated with 1.6e16 n_{eq}/cm^2 (neutrons, Ljubljana)
20 V, no cooling, I=0.23 mA

- Main junction has shifted to backside after irradiation

- Not SPA corrected

$$\frac{dN(r,z)}{dt} = \frac{\alpha I(r,z)}{\hbar\omega} + \frac{\beta_2 I^2(r,z)}{2\hbar\omega}$$

Carrier Generation equation

Irradiation introduces defects in band gap

→ single photon absorption possible
→ TPA measurements need to be corrected

e-h Plasma

- High charge carrier densities form an e-h plasma.
- Charge carriers are shielded from external electric field
- Drift of charge carriers is delayed
- Pulses appear elongated

- Onset of plasma observed ~0.3nJ / 100°NDF

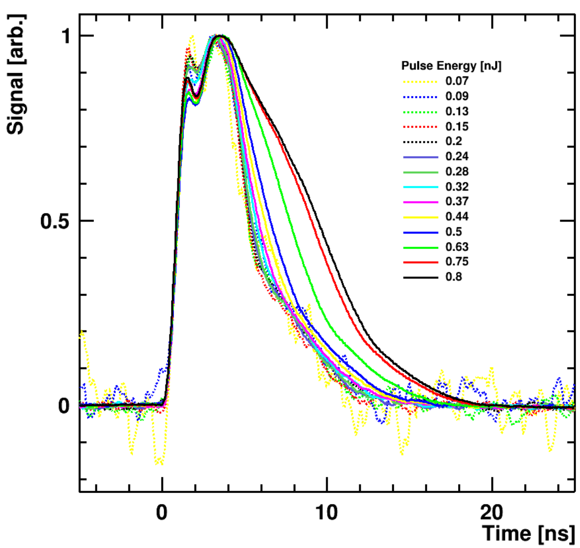

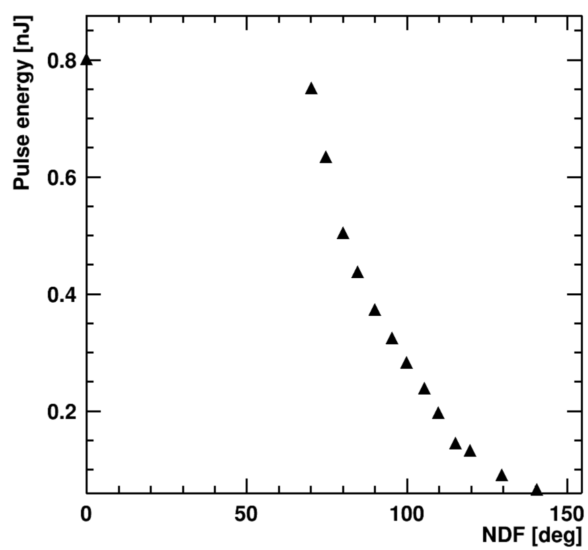

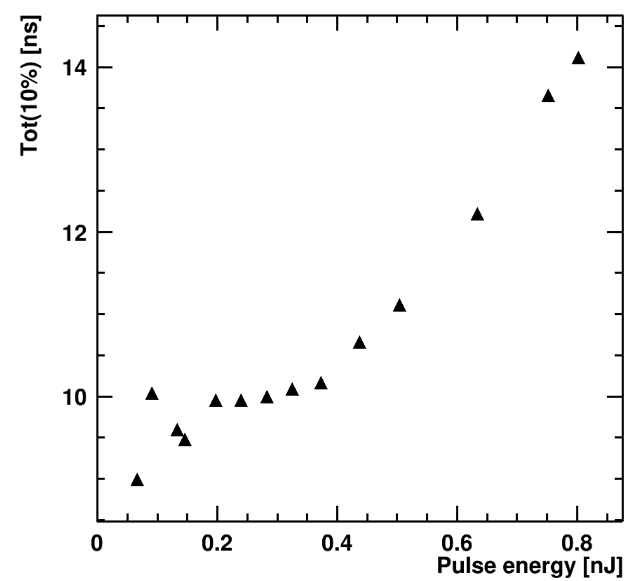

Current sensitive amplifier, BS on, 7859-WL-A63-PIN4 at 100V, 20°C

Nonlinear Optics

$$\tilde{\mathbf{D}} = \epsilon_0 \tilde{\mathbf{E}} + \tilde{\mathbf{P}}$$

$$\tilde{P}(t) = \epsilon_0 [\chi^{(1)} \tilde{E}(t) + \chi^{(2)} \tilde{E}^2(t) + \chi^{(3)} \tilde{E}^3(t) + \cdots]$$

linear interactions

second order nonlinear interactions:
- second harmonic generation (SHG)
- difference- / sum-frequency generation

only for non-centrosymmetric media

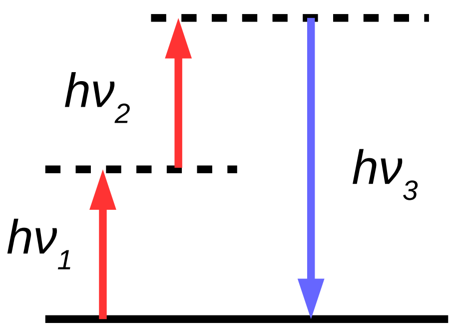

e.g. frequency-upconversion in BBO crystal by SHG

third order nonlinear interactions:
- four wave mixing, THG
- optical Kerr effect, TPA

$$n = n_0 + n_2 I$$

lowest order nonlinear interaction for centrosymmetric media (like liquids, gases, amorphous solids, silicon..)

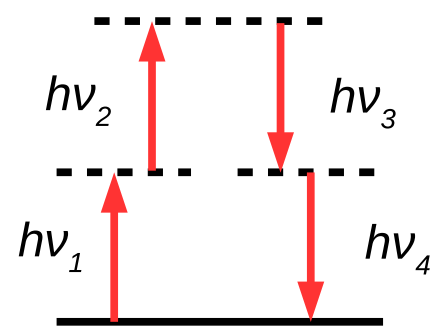

in general:
$\nu_1 \neq \nu_2 \neq \nu_3 \neq \nu_4$

degenerate case:
$\nu_1 = \nu_2 = \nu_3 = \nu_4$
Kerr effect → Re($\chi^{(3)}$)
TPA → Im($\chi^{(3)}$)

Nonlinear optics (3rd), Robert W.Boyd

Phase matching

Consider the phase of an electromagnetic wave **ωt-kr**

Sum frequency generation in general:

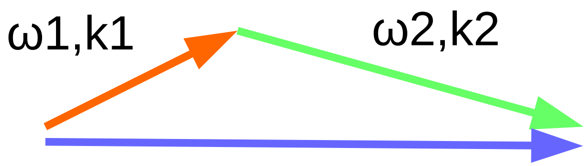

$\omega_1+\omega_2=\omega_3$
$k_1+k_2=k_3$

Second harmonic generation with collinear beams:

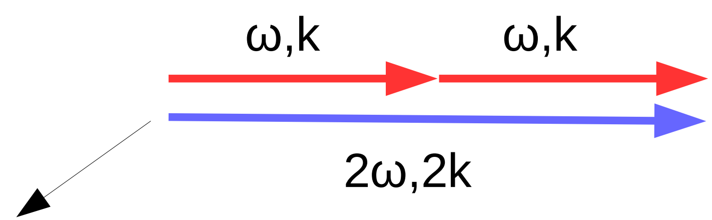

Incident wave and second harmonic need to see the same refractive index:

n(ω)=n(2ω)

But: Large ω → large n (normal dispersion)

BBO is a material with negative birefringence ($n_e < n_o$)

→ Align polarization of ω perpendicular to optical axis

→ tune n_e by turning crystal

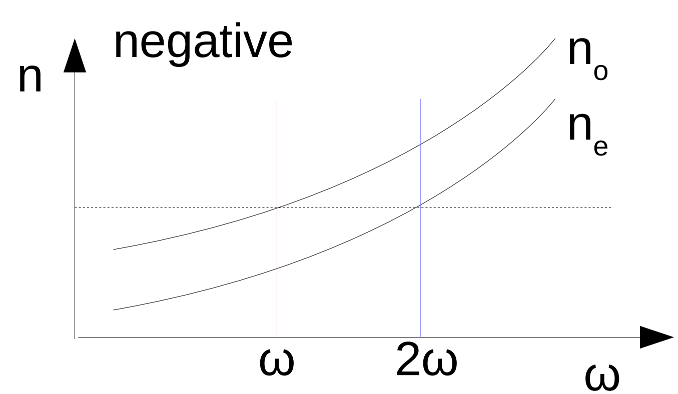

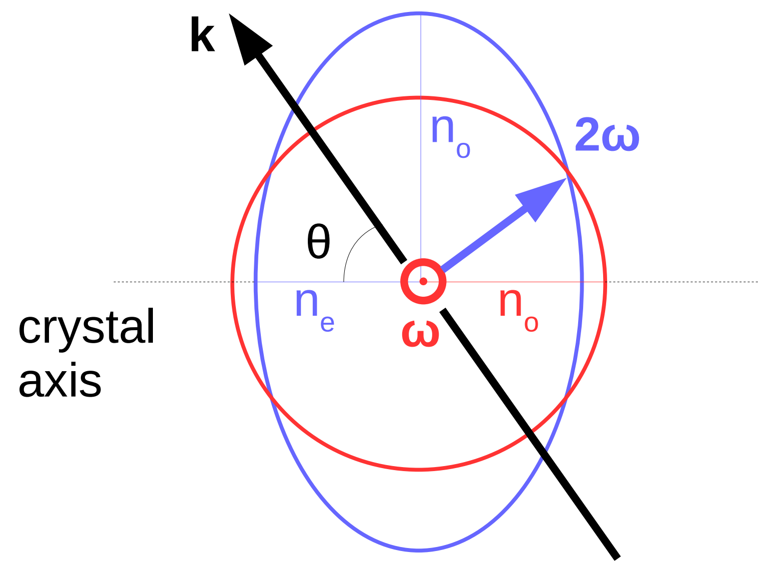

Dispersion of Short Pulses

The phase of a pulse is modified when propagating through a medium

$$E_{out}(\omega) = E_{in}(\omega) \cdot e^{-i(k(\omega)\cdot x)}$$

***x* = material width**

$$k(\omega) = n(\omega)\omega / c$$

$$k(\omega) = k(\omega_0) + k' \cdot (\omega - \omega_0) + \frac{1}{2} k'' \cdot (\omega - \omega_0)^2 + \ldots$$

Constant term: All spectral components are shifted by the same amount → no change of pulse width

Linear Term: Temporal phase still constant → pulse is delayed, no change of pulse width

Non-Linear Term: Non-linear temporal phase
Pulse is stretched: ‘chirped pulse’

Dispersion of Short Pulses

GDD: Group Delay Dispersion

Severe for (ultra) short pulses due to large spectral bandwidth!

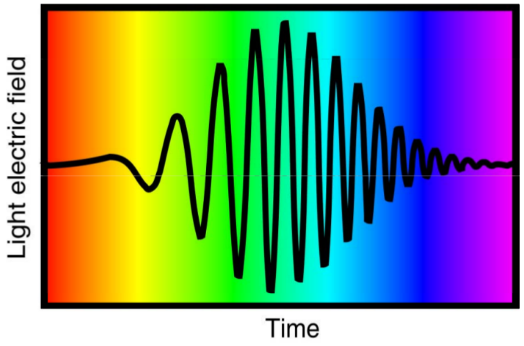

(Chirped pulse)

$\Delta t \cdot \Delta \nu > 0.44$

$$\Delta t_{out} = \frac{\sqrt{\Delta t^4 + 16(\ln 2)^2 GDD^2}}{\Delta t}$$

$$GVD = \frac{\lambda^3}{2\pi c^2}\left(\frac{\partial^2 n}{\partial \lambda^2}\right) \rightarrow GDD = L \cdot GVD$$

Material thickness L

Pulse width of a λ=800 pulse after 20mm BK 7 glass.

(GDD=1000 fs^2)

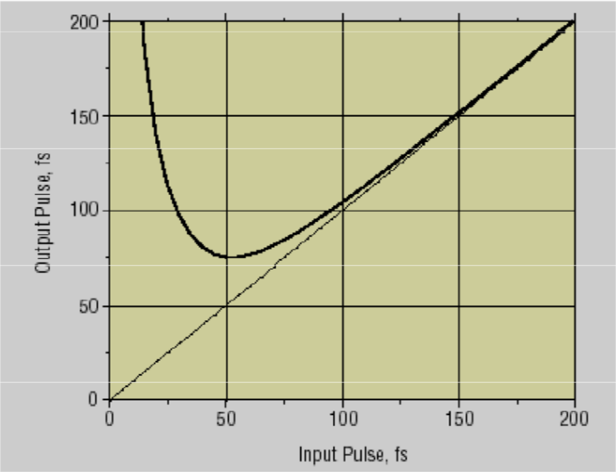

Z-scan..

This sensor is ~200µm thick

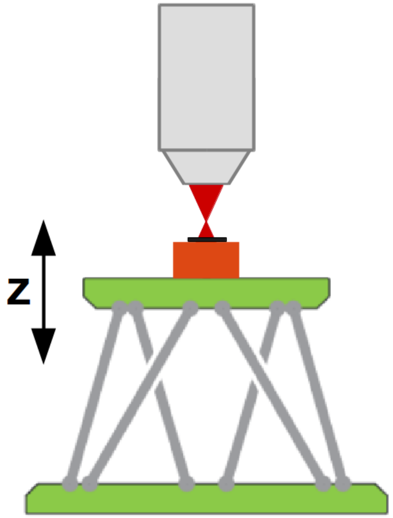

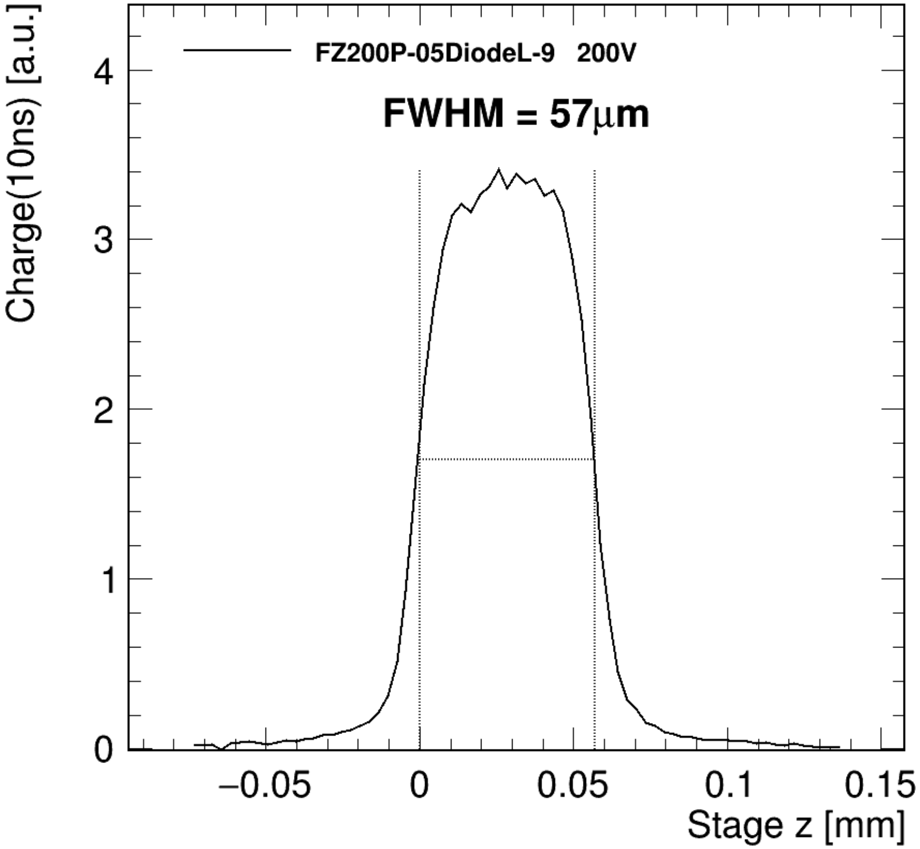

movement of positioning stage ≠ movement of focal point

Z-scaling

I. Refraction: Beam appears elongated in silicon
→ Rayleigh length z0 is different in si/air

'Scaling' of z depends on focusing optics: NA or z0
(here z0 is the value in silicon!)

$$z' = z \cdot \sqrt{\frac{z_0 \pi n^3}{z_0 \pi n - \lambda n^2 + \lambda}}$$

derived from

$$\sin\theta = n \sin\theta'$$
$$\tan\theta' = w_0/z_0$$
$$z_0 = \pi n w_0^2/\lambda$$

alternative using NA=n sinθ

$$z' = z\sqrt{\frac{n^2 - NA^2}{1 - NA^2}}$$

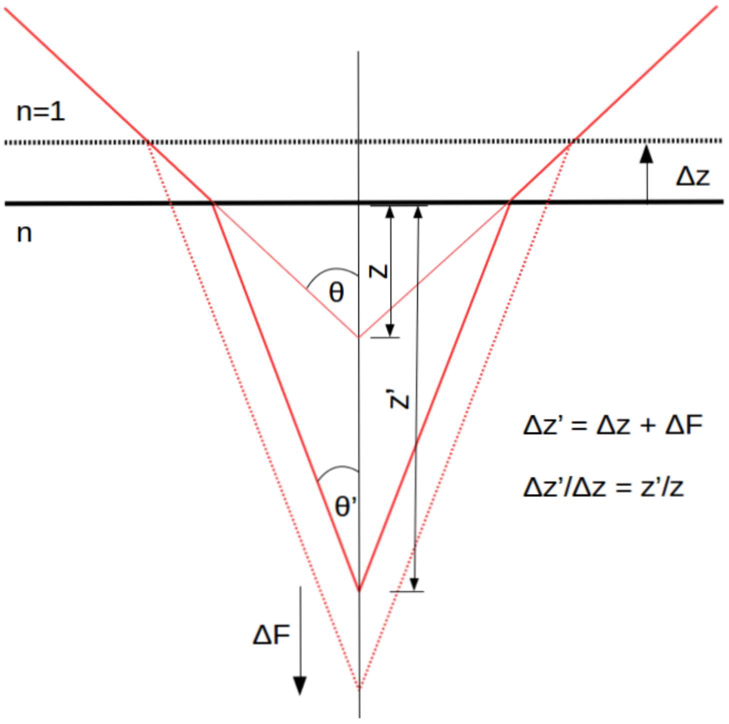

II. Stage movement by Δz
→ focal point movement ΔF

focal point to sensor surface changes by
Δz' = Δz + ΔF

same scaling applies for Δz to Δz' as for z to z'

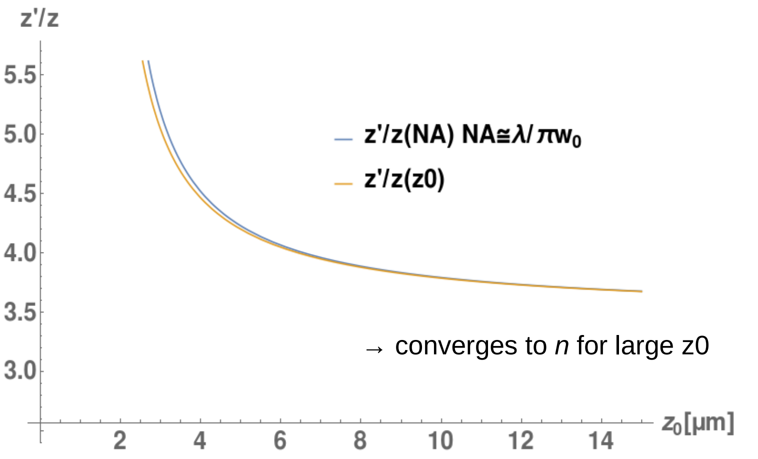

Z-scan

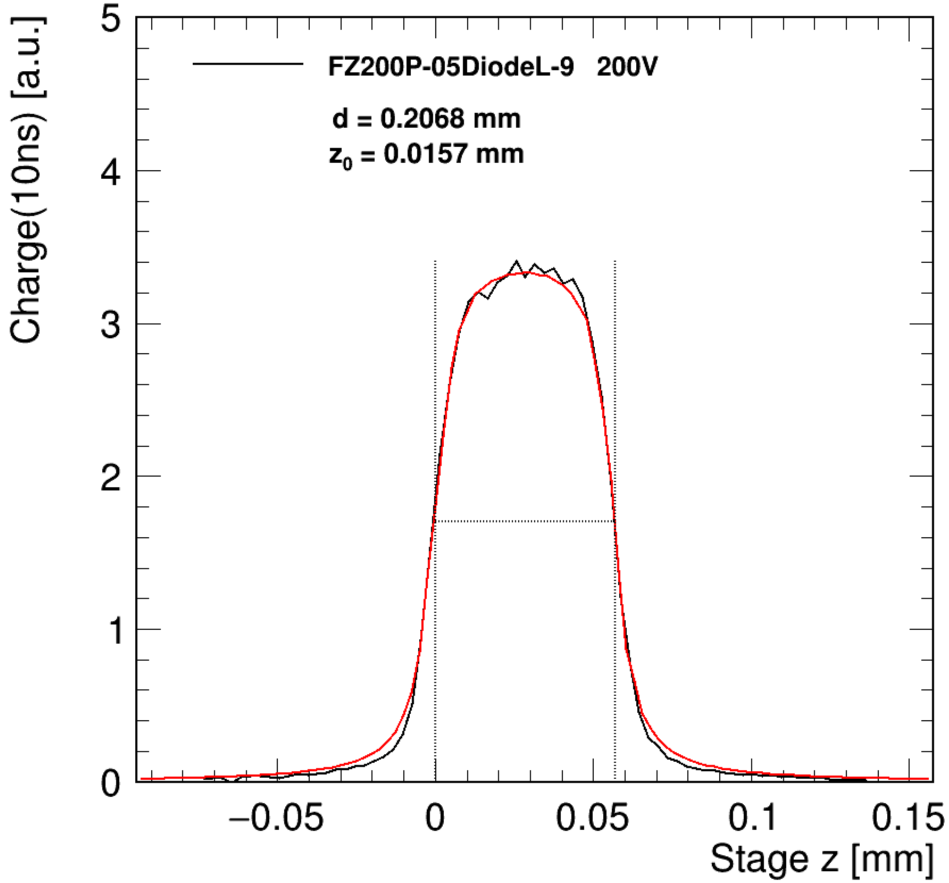

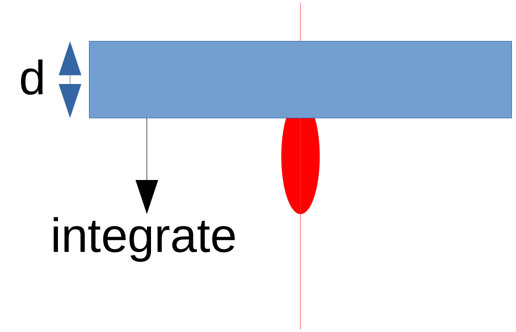

Fit with:

$$N^d_{tpa}(z) = 2\pi \int_{z-d}^{z} \int_0^{\infty} n_{tpa}(r, z')\, r dr\, dz'$$

$$= \frac{E_p^2\, n^2\, \beta_2\, \sqrt{\ln 4}}{4\, c\, \hbar\, \pi^{\frac{3}{2}}\, \tau} \cdot \left[\tan^{-1}\left(\frac{(d-z)}{z_0}\right) + \tan^{-1}\left(\frac{z}{z_0}\right)\right]$$

- account for refraction: replace z → z'
- d [mm] is sensor thickness
- z0 is the Rayleigh length in silicon

$$z' = z \cdot \sqrt{\frac{z_0\, \pi n^3}{z_0 \pi n - \lambda n^2 + \lambda}}$$

Technicality:
Horizontal axis not scaled to include z0 into fit

Result
d = 207µm
z0 = 15.7µm → w0 = 1.5µm
$NA = n \sin\theta \approx \lambda / \pi w_0$ = 0.33

d as expected
CV measurement: 209µm

but nominal NA=0.5
→ w0 = 1µm, z0 = 6.9µm
→ focusing not as good as it could be?

Additional Use-case for TPA

CERN Electronic Systems for Experiments (CERN-EP-ESE)

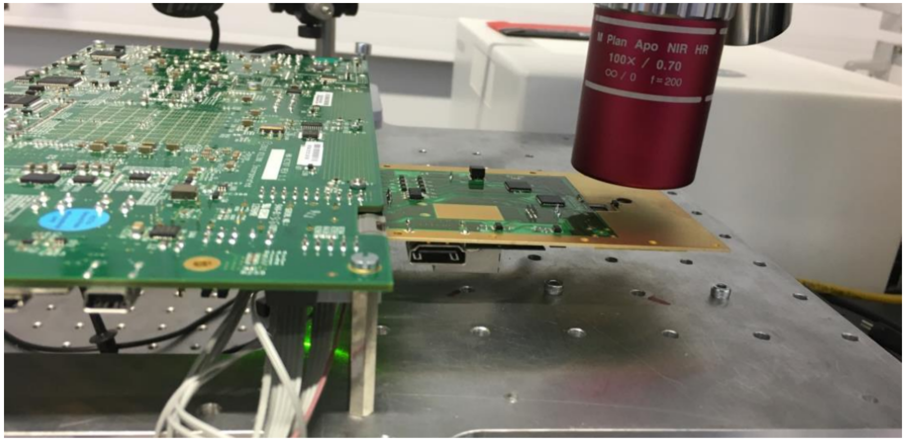

Single Event Upset (SEU) test with TPA, performing measurements in Montpellier

Can this be done at CERN with TPA-TCT-setup?

Method:
- flip electronics chip upside-down
- image chip with IR illumination/camera
- perform high spatial precision SEU test

Requirement for CERN TPA-TCT-setup:
- employ IR microscopy

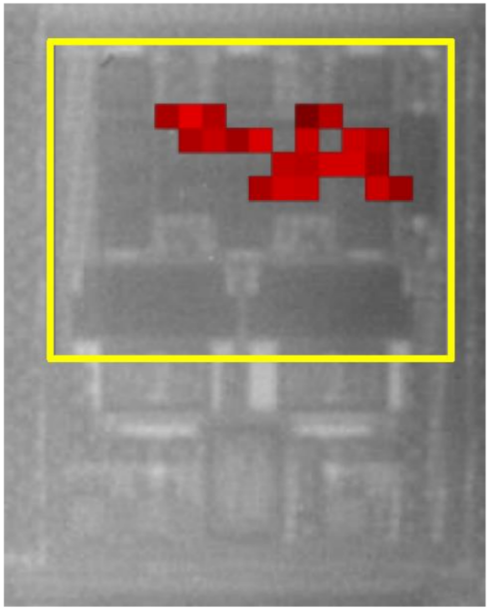

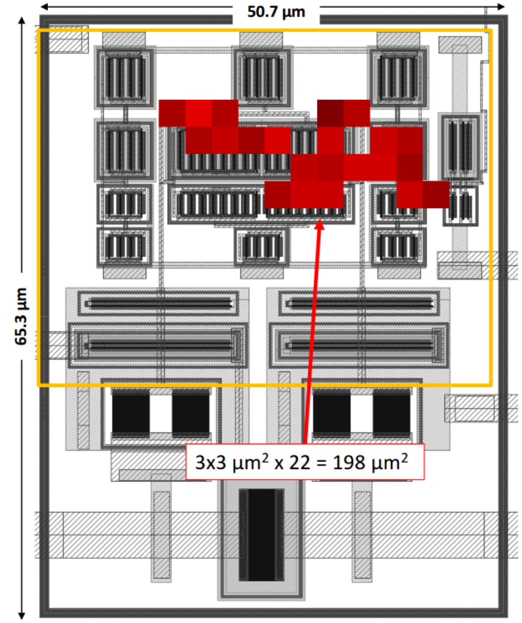

Montpellier Laser Scan Results
X. Llopart, CERN Electronic Systems for Experiments

IR + VIS Microscopy

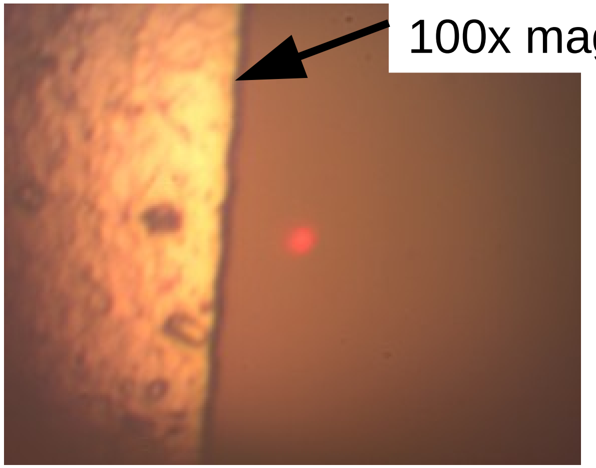

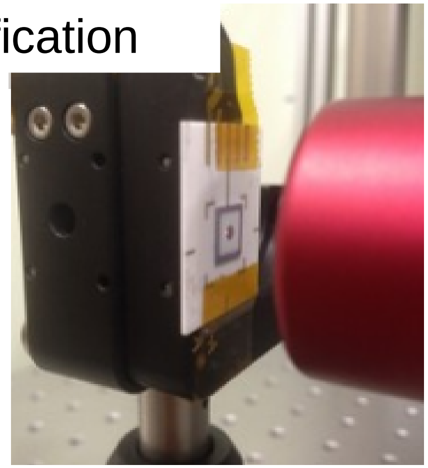

planned components for IR image in red

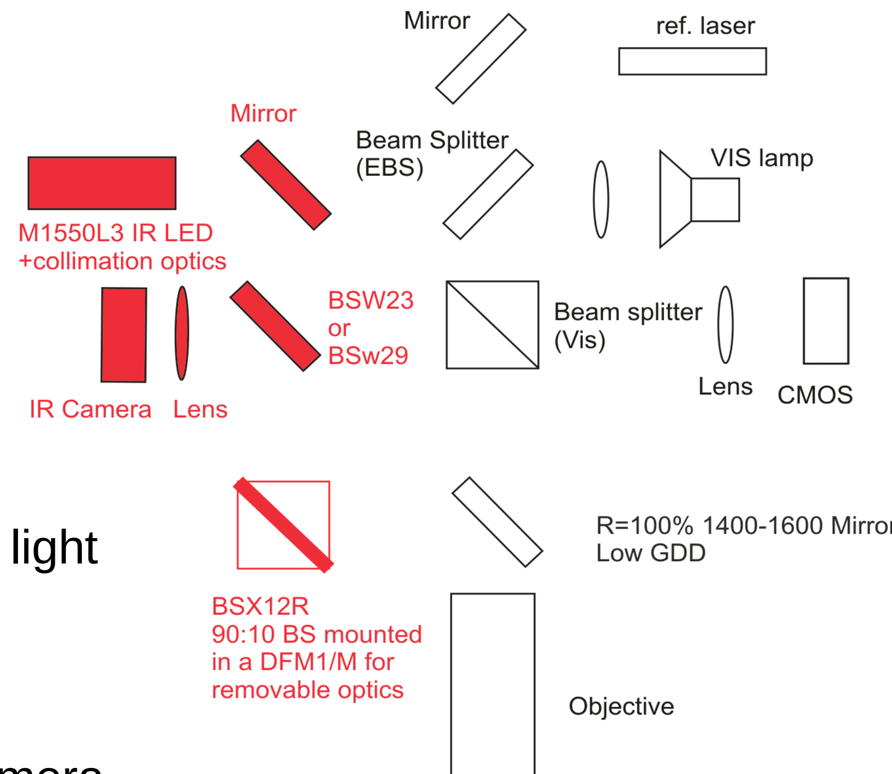

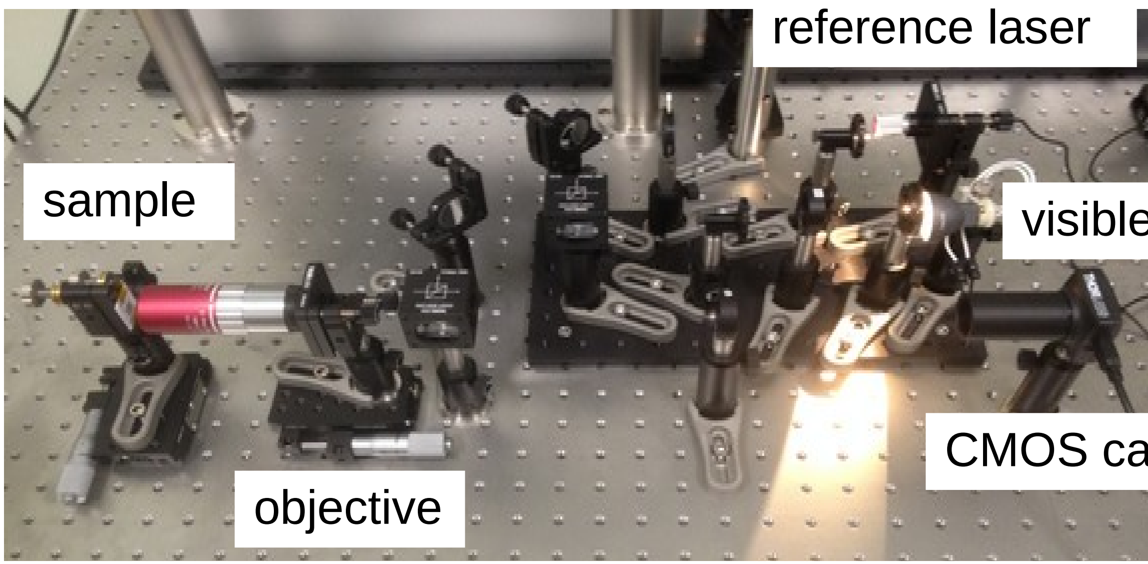

microscope setup mounted on optical table for educational purposes

IR microscope

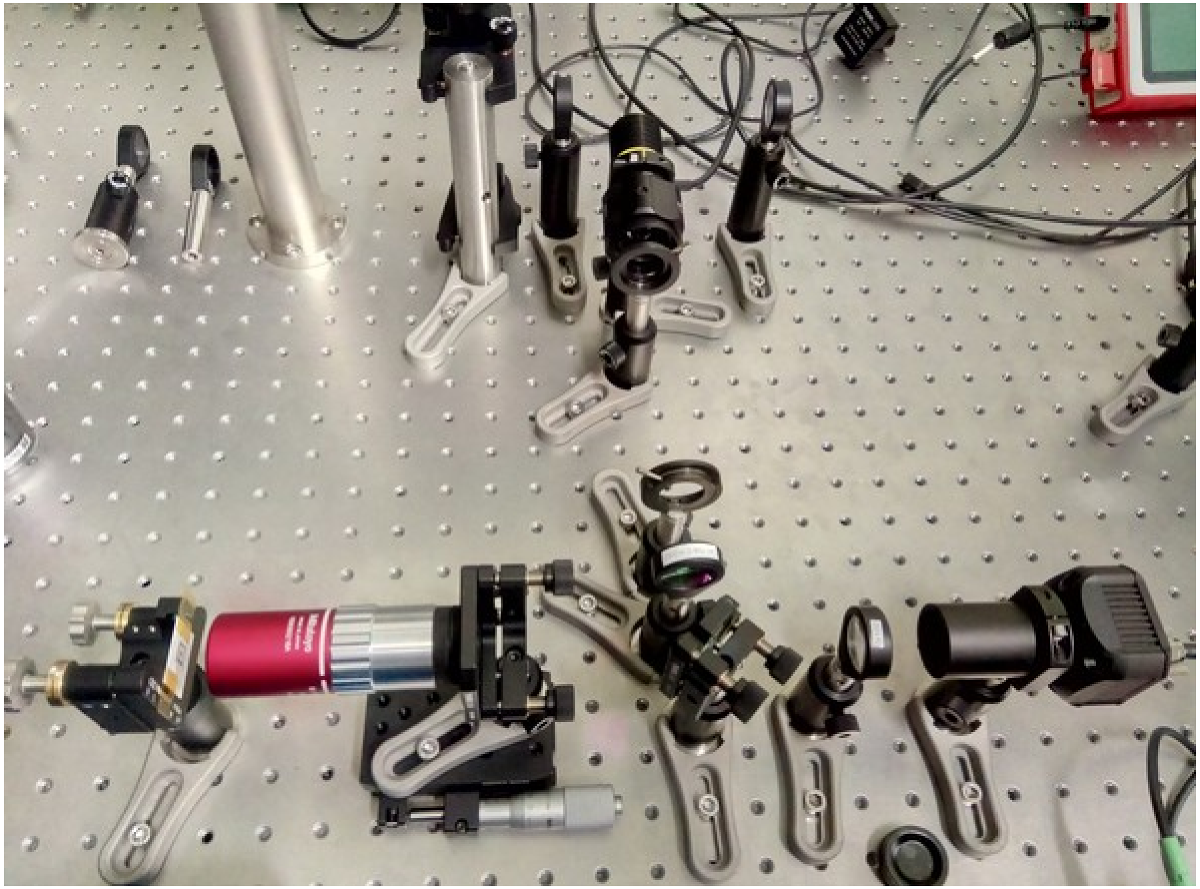

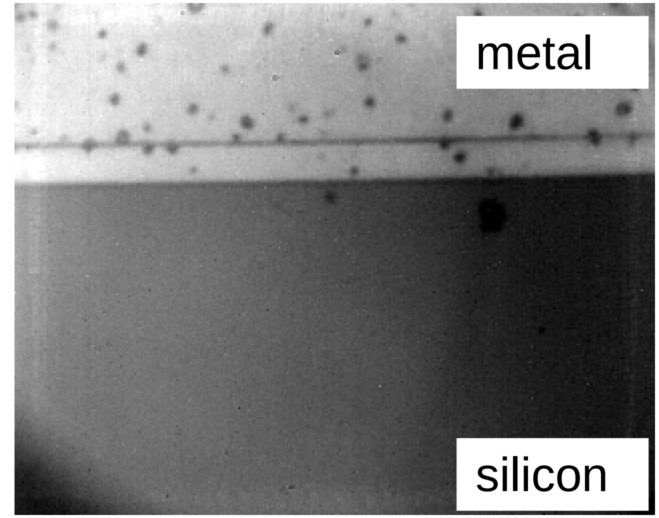

sensor top side

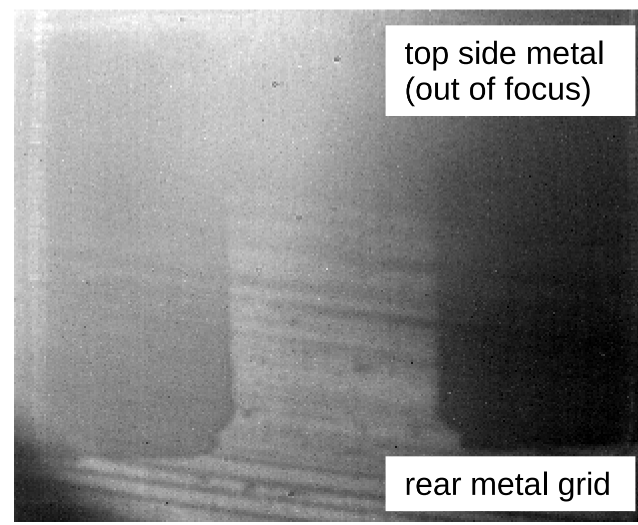

sensor rear side

note: images taken at same x/y-position, only focus was changed

IR rear imaging through bulk

	low magnification	high magnification	visible light microscope (device similar)
image from top	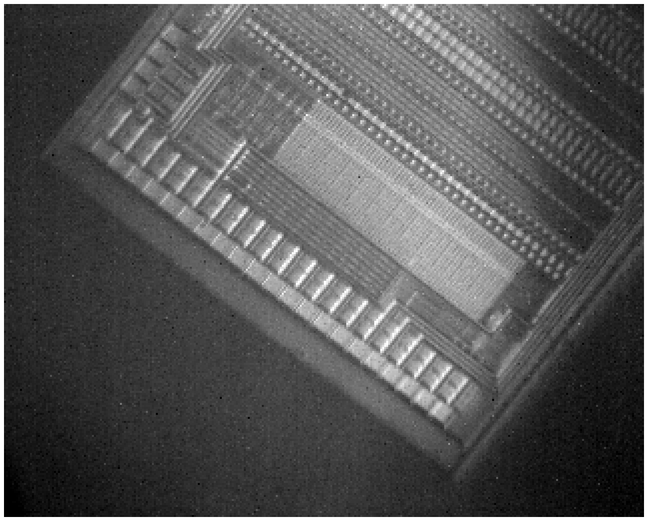	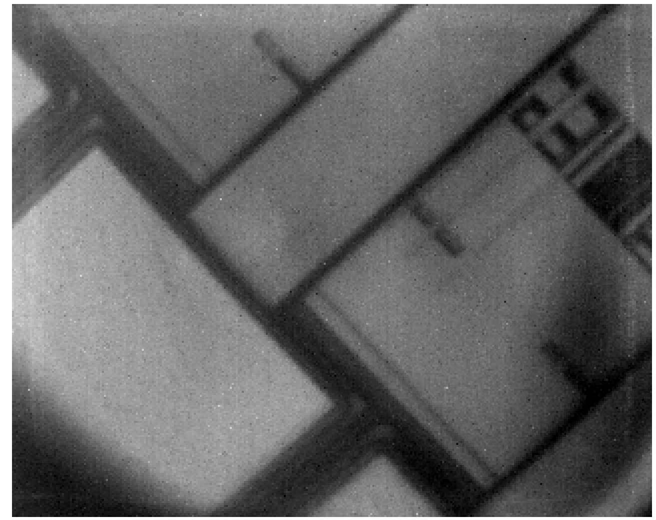	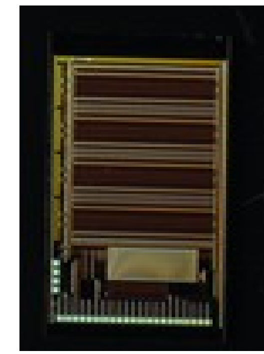
image from rear through bulk	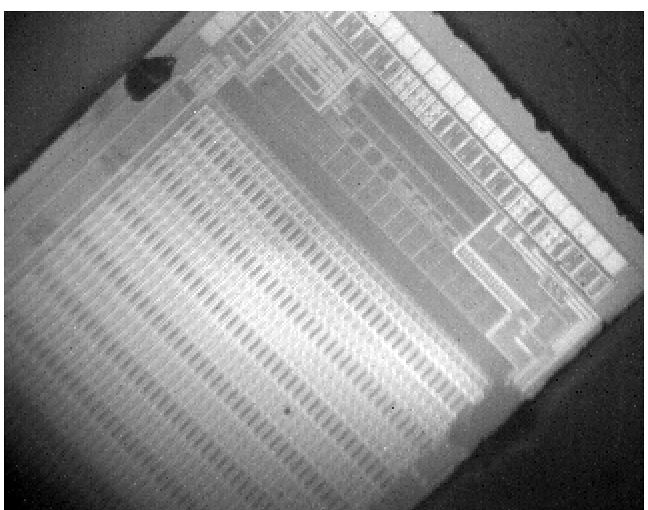		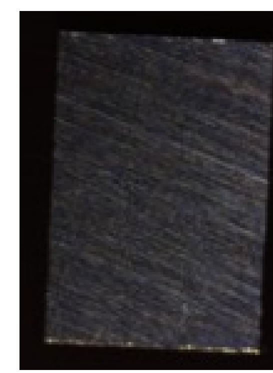

Reminder: Silicon Particle Detectors

- **Reverse biased pn-junction**
  Space charge region in depleted bulk
- **Charged particles lose energy** in material by ionization, **create electron-hole-pairs** by exciting electrons into the conduction band
- electrons / holes drift in e-field to electrodes, **drift current creates the signal (Ramo-Theorem)**

+ segmentation + read-out + V-supply + cooling etc.
+ stack detectors in several layers

→ **Tracking of charged particles**

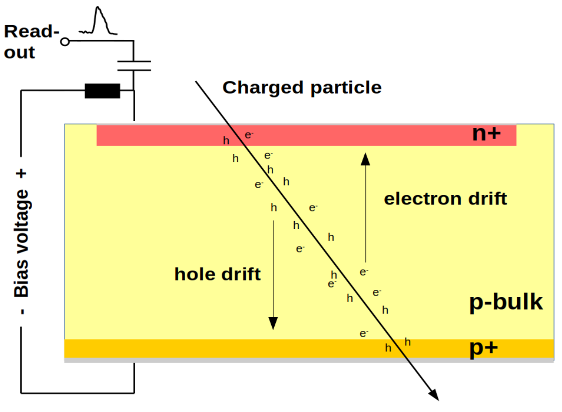

some engineering

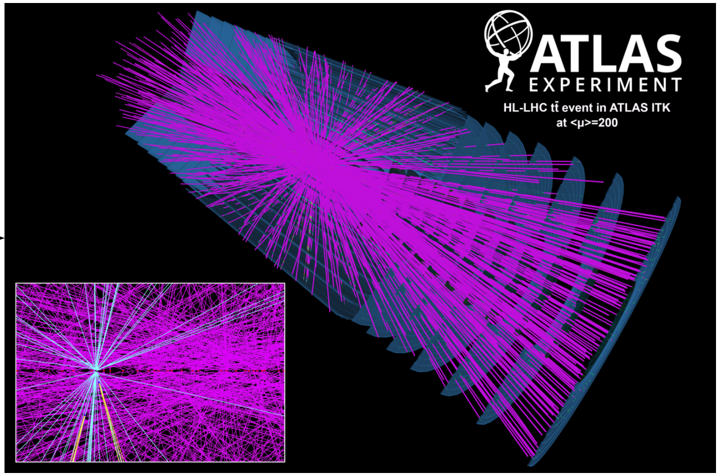

- **Radiation damage reduces sensor performance**

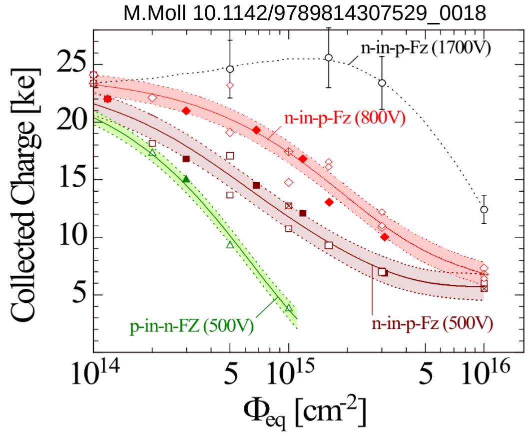

RD50 collaboration
(@CERN: EP-DT SSD-team)

“Build silicon detector with higher radiation hardness”:
- Material engineering
- Device engineering
- Characterization tools

TCT - Transient Current Technique

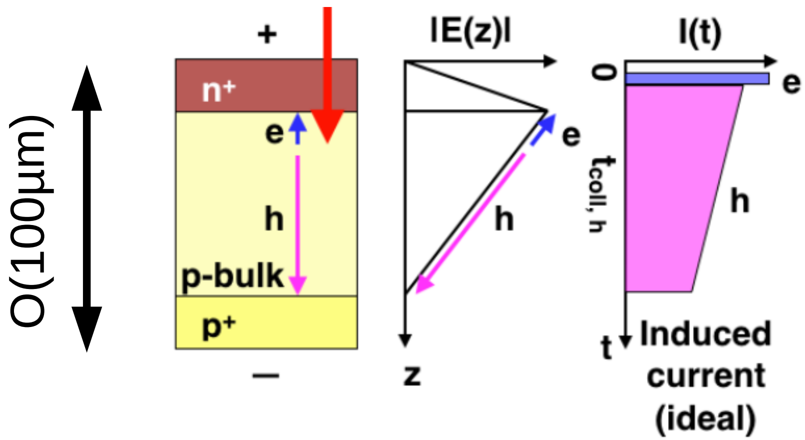

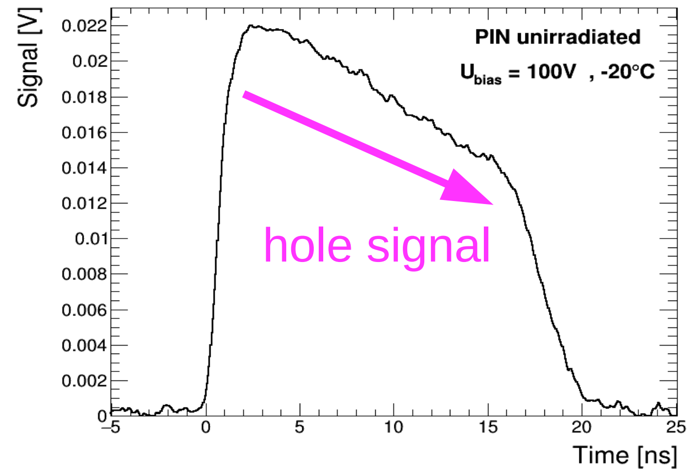

Red 660nm

Near IR 1064nm
edge-TCT

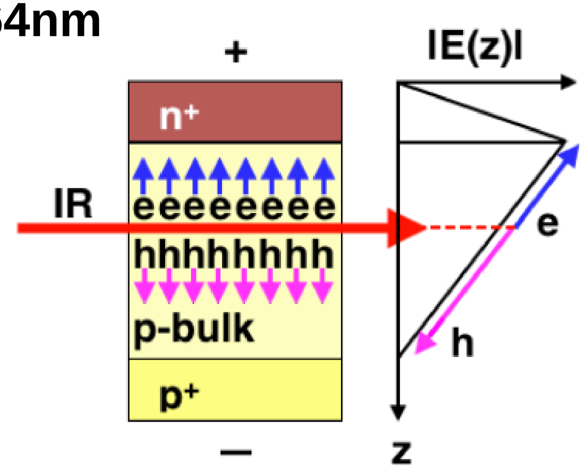

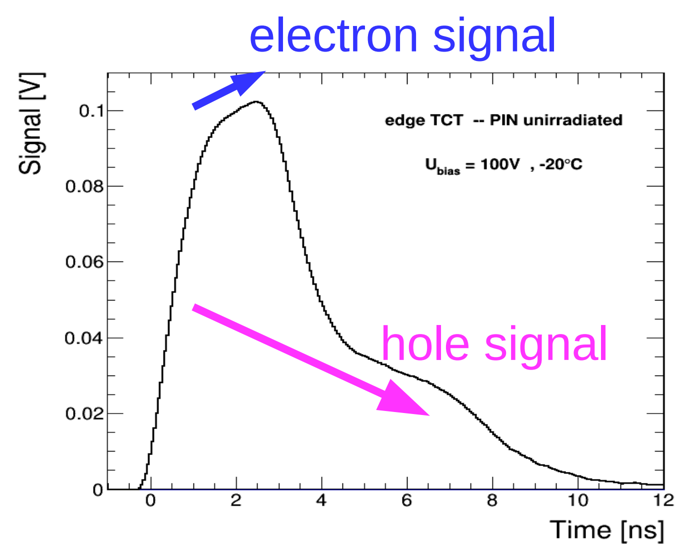

DT seminar: M. Fernández, The Transient Current Technique: laser characterization of silicon detectors https://indico.cern.ch/event/684193/
C. Gallrapp, The TCT+ setup - a system for TCT, eTCT and timing measurements, 1st TCT Workshop (2015)